C. R. Palevol 10 (2011) 381–402

Contents lists available at ScienceDirect

Comptes Rendus Palevol

www.sciencedirect.com

Evolution (Evolutionary processes, microevolution)

# Bone microanatomy and lifestyle: A descriptive approach

## *La microanatomie osseuse et le mode de vie : une approche descriptive*

Michel Laurin*, Aurore Canoville , Damien Germain

*UMR 7207, CNRS/MNHN/UPMC, département histoire de la terre, Muséum national d'histoire naturelle, "centre de recherches sur la paléobiodiversité et les paléoenvironnements", bâtiment de géologie, case postale 48, 57, rue Cuvier, 75231 Paris cedex 05, France*

ARTICLE INFO

*Article history:*
Received 15 November 2010
Accepted after revision 8 February 2011
Available online 7 April 2011

Written on invitation of the Editorial Board

*Keywords:*
Paleontology
Vertebrates
Tetrapods
Histology
Microanatomy
Ecology
Paleoecology
Long bones

ABSTRACT

Starting in 2004, our lab has published several studies on the relationship between bone microanatomy, lifestyle (aquatic to terrestrial), and the phylogeny of tetrapods. These studies emphasized quantitative and statistical analyses. Therefore, the raw data used in these studies were never published. This is unfortunate because no model captures all information in biological data. This paper remedies this situation by providing the detailed anatomical drawings used in our previous studies. These constitute the largest set of standardized cross-section images of appendicular long bones (tibiae, radii, and humeri) ever published, at least as far as the number of represented species (over one hundred) is concerned. All major aquatic to terrestrial extant tetrapod clades are represented (lissamphibians, mammals, turtles, squamates, and crocodilians). The comparative figures show that aquatic tetrapods differ most from the others, whereas amphibious taxa differ much less from their terrestrial relatives.



*Mots clés :*
Paléontologie
Vertébrés
Tétrapodes
Histologie
Microanatomie
Écologie
Paléoécologie
Os longs

RÉSUMÉ

Depuis 2004, notre laboratoire a publié plusieurs études sur la relation entre la microanatomie, le mode de vie (aquatique à terrestre), et la phylogénie des tétrapodes. Ces études privilégiaient des analyses quantitatives et statistiques. Les données brutes utilisées demeurent donc inédites. Cela est regrettable, car aucun modèle ne capture toute l'information contenue dans des données biologiques. Cette contribution remédie à cette situation, en fournissant les dessins anatomiques détaillés qui furent utilisés dans nos études antérieures. Elle présente donc la série d'illustrations de sections transversales d'os longs appendiculaires (tibias, radius et humérus) la plus exhaustive jamais publiée, au moins par le nombre d'espèces (plus d'une centaine) concernées. Tous les grands clades de tétrapodes actuels, aquatiques à terrestres, sont représentés (lissamphibiens, mammifères, tortues, squamates, et crocodiliens). Les illustrations comparatives montrent que les tétrapodes aquatiques diffèrent le plus des autres, alors que les taxons amphibies diffèrent moins fortement de leurs proches parents terrestres.



## 1. Introduction

A relationship between bone microanatomy and lifestyle (aquatic to terrestrial) has long been documented

* Corresponding author.
*E-mail address:* michel.laurin@upmc.fr (M. Laurin).

1631-0683/$ – see front matter © 2011 Académie des sciences. Published by Elsevier Masson SAS. All rights reserved.
doi:10.1016/j.crpv.2011.02.003

(e.g. Fish and Stein, 1991; Stein, 1989; Wall, 1983). Study of this relationship is useful both to determine how bone microanatomy evolves in response to habitat shifts (e.g. de Buffrénil et al., 2010; Kriloff et al., 2008) and to infer the habitat of early vertebrates (de Ricqlès, 1974a, 1974b; Germain and Laurin, 2005; Nopcsa and Heidsieck, 1934; Steyer et al., 2004). Most studies in this field have investigated bone compactness or density (Fish and Stein, 1991; Stein, 1989; Wall, 1983). In contrast, we have used a more complex compactness profile model to capture more information about bone sections (Girondot and Laurin, 2003; Laurin et al., 2004). That model is presented in detail elsewhere (Girondot and Laurin, 2003; Laurin et al., 2004), so it is enough to note that it carries information about the compactness near the center of the bone (hence, of the medullary spongiosa) and about cortical compactness, hence, about the cortico-diaphyseal index (Castanet et al., 2000), among other things.

In previous studies, we have reported analyses about body size and quantitative attributes of bone microanatomy captured by our model. The analyses were based on inter-specific datasets that included between 37 (Canoville and Laurin, 2009) and 99 (Kriloff et al., 2008) species (mostly extant) of known lifestyle. The sample included lissamphibians (Canoville and Laurin, 2009; Laurin et al., 2004, 2009), amniotes (Canoville and Laurin, 2010; Germain and Laurin, 2005), or both (Kriloff et al., 2008). The statistical tests used exploited phylogenetic information. The first statistical technique (Germain and Laurin, 2005; Laurin et al., 2004) was a multiple regression on distance matrices (including a phylogenetic distance matrix) with permutations to test the significance, which is basically a modified Mantel test (Mantel, 1967). However, Legendre (Legendre, 2000) showed that correlation tests performed on distance matrices are less powerful than on the original, untransformed variables. Thus, for subsequent studies (Canoville and Laurin, 2009; Canoville and Laurin, 2010; Kriloff et al., 2008; Laurin et al., 2009), we used a variance partitioning technique with PVR (Phylogenetic eigenVector Regression) in which the phylogeny is represented by selected axes of principal coordinates derived from the distance matrix (Desdevises et al., 2003). We initially refrained from using the now classical phylogenetically independent contrasts (FIC) (Felsenstein, 1985) because that method was developed for continuous variables, whereas the lifestyle is usually treated as a discrete variable. To make matters worse, amphibious taxa are not phenotypically intermediate between aquatic and terrestrial taxa (e.g. Canoville and Laurin, 2010; Laurin et al., 2004), preventing an ordered, ternary coding of lifestyle to be used directly in FIC analysis. However, FIC analysis was performed on parts of our dataset by coding the habitat as a binary variable (Canoville and Laurin, 2010; Laurin et al., 2009). All these analyses corroborated the long-established consensus that bone microanatomy includes information on the lifestyle (e.g. Fish and Stein, 1991; Stein, 1989; Wall, 1983), although we believe that we were the first to demonstrate that using phylogenetically-informed statistical tests.

Globally, our tests suggest that aquatic taxa have either more compact bones than amphibious and terrestrial taxa, as in lissamphibians (Canoville and Laurin, 2009; Laurin et al., 2004; Laurin et al., 2009), or more spongy medullary bone, but not necessarily higher compactness, as in amniotes (Canoville and Laurin, 2010; Germain and Laurin, 2005; Kriloff et al., 2008). The greater compactness of long bones aquatic lissamphibians results from a thicker cortex, from a medullary spongiosa (observed mostly in large forms), or from a combination of both. In pelagic forms, the cortex can actually be less compact than in terrestrial forms. Aquatic taxa also tend to have a more gradual transition between cortical compacta and medullary spongiosa (or medullary region, when devoid of spongiosa) than amphibious taxa.

Unfortunately, most of the primary data supporting these conclusions, namely detailed anatomical drawings of long bone cross-sections, remain unpublished, due to space constraints in most journals that emphasize quantitative analyses; given the space required to present methods and results of the statistically-oriented papers, no space was available to publish the bulk of the illustrations. Only drawings of the sections on lissamphibian humeri (Canoville and Laurin, 2009) and femora (Laurin et al., 2009) have been published (along with selected pictures of a higher magnification showing bone histology). Making these illustrations available is important for several reasons. First, no model can capture all information present in raw data. These drawings will allow future reanalyses when better, more sophisticated models become available. Second, not all morphologists are equally comfortable with numbers, equations, and statistics, and some may prefer visually assessing the validity of our conclusions using the drawings. Indeed, informal conversations with various colleagues suggested that several were not familiar with our statistical methods and prompted one of us to explain them more fully in a paper specially dedicated for this purpose (Laurin et al., 2006). Although many studies have published images of cross-sections of long bones, very few have done so for a large number of taxa, and at a standardized level (here, mid-diaphyseal). Below, we present what we believe is the largest comparative dataset of extant tetrapod long bone cross-sections ever published. These images may also prove useful as a basis for comparison when drawing paleobiological inferences using relatively simple numerical methods (Mukherjee et al., 2010; Ray et al., 2005), rather than statistically validated inference models (Canoville and Laurin, 2009, 2010; Germain and Laurin, 2005; Kriloff et al., 2008; Laurin et al., 2004, 2009) (although we encourage use of the latter). Third, these data may contain systematically relevant characters that we have so far overlooked because the primary focus of our papers has been paleobiological and adaptative. All our tests suggest a strong phylogenetic signal in these data (Canoville and Laurin, 2009, 2010; Germain and Laurin, 2005; Kriloff et al., 2008; Laurin et al., 2004, 2009), but we have not tried identifying apomorphies of various clades. Thus, publication of these drawings may have a systematic interest.

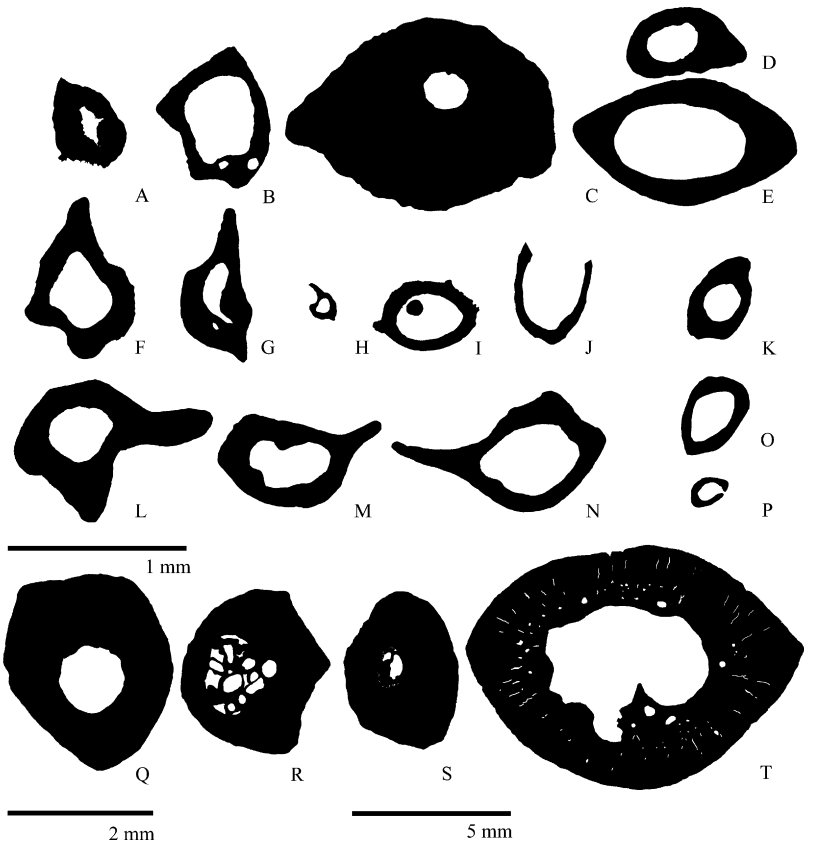


**Fig. 1.** Mid-diaphyseal cross-sections of lissamphibian tibiae. Urodeles (**A–S**) and anurans (**T**) with tibiae of small (**A–P**), medium (**Q–R**) and large diameter (**S–T**). These include aquatic (**A–E, Q–S**), amphibious (**F–H**) and terrestrial (**I–P, T**) taxa. Figure parts reflect lifestyle, tibial diameter, and phylogenetic affinities. Taxa illustrated are: **(A)** *Onychodactylus fischeri;* **(B)** *Ambystoma mexicanum* (subadult); **(C)** *Necturus maculosus;* **(D)** *Proteus anguineus*; **(E)** *Amphiuma means;* **(F)** *Pleurodeles waltl;* **(G)** *Triturus cristatus;* **(H)** *Triturus alpestris;* **(I)** *Salamandrella keyserlingii;* **(J)** *Ambystoma opacum;* **(K)** *Plethodon glutinosus;* **(L)** *Salamandra lanzai;* **(M)** *Salamandra atra;* **(N)** *Salamandra salamandra;* **(O)** *Desmognathus monticola;* **(P)** *Desmognathus ochrophaeus;* **(Q)** *Ambystoma andersoni;* **(R)** *Cryptobranchus alleganiensis;* **(S)** *Andrias japonicus*; **(T)** *Leptodactylus pentadactylus* (Anura). Scale: (**A–P**): 1 mm; (**Q–R**): 2 mm; (**S–T**): 5 mm.
**Fig. 1.** Coupes transversales mi-diaphysaires de tibias de lissamphibiens. Urodèles (**A–S**) et anoures (**T**) dont le tibla est de petit (**A–P**), moyen (**Q–R**) et grand diamètre (**S–T**). Ceux-ci incluent des taxons aquatiques (**A–E, Q–S**), amphibies (**F–H**), et terrestres (**I–P, T**). Les taxons sont disposés selon leur mode de vie, le diamètre de leur tibia et la taxonomie. Les taxons représentés sont : **(A)** *Onychodactylus fischeri ;* **(B)** *Ambystoma mexicanum* (subadulte) ; **(C)** *Necturus maculosus* ; **(D)** *Proteus anguineus* ; **(E)** *Amphiuma means* ; **(F)** *Pleurodeles waltl* ; **(G)** *Triturus cristatus* ; **(H)** *Triturus alpestris* ; **(I)** *Salamandrella keyserlingii* ; **(J)** *Ambystoma opacum* ; **(K)** *Plethodon glutinosus* ; **(L)** *Salamandra lanzai* ; **(M)** *Salamandra atra* ; **(N)** *Salamandra salamandra* ; **(O)** *Desmognathus monticola* ; **(P)** *Desmognathus ochrophaeus* ; **(Q)** *Ambystoma andersoni* ; **(R)** *Cryptobranchus alleganiensis* ; **(S)** *Andrias japonicus* ; **(T)** *Leptodactylus pentadactylus* (Anura). Échelle : (**A–P**) : 1 mm; (**Q–R**) : 2 mm; (**S–T**) : 5 mm.

## 2. Methods

All illustrations presented below were used to perform the statistical tests in our previous publications (Canoville and Laurin, 2009, 2010; Germain and Laurin, 2005; Kriloff et al., 2008; Laurin et al., 2004, 2009). Thus, no new statistical tests are performed here, both because results of these tests are already reported in our previous papers, and to save space to present and describe the drawings. All sections are of adults or subadults, to the extent that this could be determined. The illustrations were produced with a camera lucida, or were drawn by computer using Adobe Photoshop© from a digital picture, or represent edited radiographs. For the source of the material, see the original papers. The figures were organized according to a combination of taxonomic, ecological, and size criteria. Thus, most figures represent extant lissamphibians, mammals, turtles, or diapsids. The taxonomic order in which taxa are presented and our use of the word "diapsid" reflect the traditional position of turtles outside Diapsida, as supported by morphological (Laurin and Reisz, 1995; Lee, 1997; Lyson et al., 2010; Reisz and Laurin, 1991), "total evidence" (Frost et al., 2006; Lee, 2001), or developmental data (Werneburg and Sánchez–Villagra, 2009), despite the fact that most molecular (Hedges and Poling, 1999; Hugall et al., 2007; Iwabe et al., 2005) and some paleontological analyses (deBraga and Rieppel, 1997; Rieppel and Reisz, 1999) place turtles within Diapsida. In any case, at least some turtle specialists acknowledge that this is an unresolved problem (Sterli, 2010). This decision is further justified by the fact that turtles appear to display a different and weaker pattern of covariation between bone microanatomy and habitat than other amniotes, as previously noted (Canoville and Laurin, 2010; Germain and Laurin, 2005; Kriloff et al., 2008). However, using another reference taxonomy would not

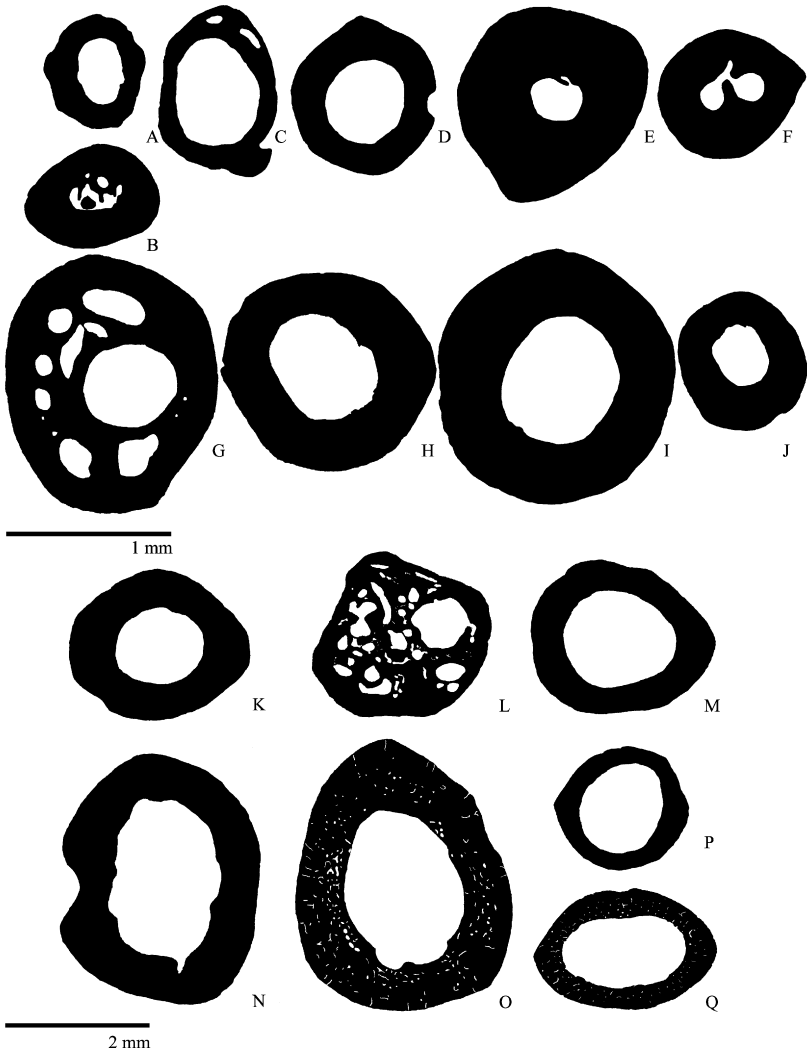


**Fig. 2.** Mid-diaphyseal cross-sections of tibiae of small-sized (**A–J**) and medium-sized (**K–Q**), aquatic (**A–B, K–L**), amphibious (**C–F, M**) and terrestrial (**G–J, N–Q**) anurans. Taxa are arranged according to their body size, lifestyle and phylogenetic affinities. Taxa illustrated are: **(A)** *Bombina orientalis;* **(B)** *Pipa carvalhoi;* **(C)** *Lithobates forreri;* **(D)** *Rana iberica;* **(E)** *Discoglossus* sp.; **(F)** *Ascaphus truei;* **(G)** "*Bufo" pentoni;* **(H)** *Rana dalmatina;* **(I)** *Pachymedusa dacnicolor;* **(J)** *Chiromantis rufescens;* **(K)** *Telmatobius culeus;* **(L)** *Xenopus laevis;* **(M)** *Lithobates vaillanti;* **(N)** *Epidalea calamita;* **(O)** *Rhinella marina*; **(P)** *Hypsiboas boans;* **(Q)** *Ceratophrys aurita.* Scale: (**A–J**): 1 mm; (**K–Q**): 2 mm.

**Fig. 2.** Coupes transversales mi–diaphysaires de tibias d'anoures de petite (**A–J**) et moyenne tailles (**K–Q**), aquatiques (**A–B, K–L**), amphibies (**C–F, M**), terrestres (**G–J, N–Q**). Les taxons sont disposés selon leur mode de vie et leur ordre dans la phylogénie. Les taxons représentés sont : **(A)** *Bombina orientalis ;* **(B)** *Pipa carvalhoi ;* **(C)** *Lithobates forreri ;* **(D)** *Rana iberica ;* **(E)** *Discoglossus* sp. ; **(F)** *Ascaphus truei ;* **(G)** "*Bufo" pentoni* ; **(H)** *Rana dalmatina* ; **(I)** *Pachymedusa dacnicolor* ; **(J)** *Chiromantis rufescens* ; **(K)** *Telmatobius culeus* ; **(L)** *Xenopus laevis* ; **(M)** *Lithobates vaillanti* ; **(N)** *Epidalea calamita* ; **(O)** *Rhinella marina* ; **(P)** *Hypsiboas boans* ; **(Q)** *Ceratophrys aurita.* Échelle : (**A–J**) : 1 mm; (**K–Q**) : 2 mm.

alter our conclusions. Within each of the four main taxa, it was sometimes necessary to present separately relatively small (and mid-sized) bones and relatively large ones because showing all at the same scale would make bones of the taxa of small body size so minute that no detail would be visible. Finally, within these four taxa and size groups, aquatic taxa are placed in the upper row(s), followed by amphibious taxa, and then by terrestrial ones, to facilitate comparisons between ecological categories. Birds have been excluded here and from our previous studies because flight and air sacs induce strong constraints that would a priori complicate comparisons.

## 3. Structure and functional interpretation of tetrapod long bones: tibia

Urodeles often retain gilled aquatic larvae (Hanken, 1999), such as those that existed in seymouriamorphs (Laurin, 2000) and at least some temnospondyls (Fröbisch and Schoch, 2009) and that may represent a primitive attribute of stegocephalians (e.g. Laurin, 2008). They display the full range of lifestyles, from purely aquatic in cryptobranchids, sirenids, and amphiumids, to fully terrestrial in some plethodontids and some salamandrids. Their tibial microanatomy reflects this to an extent, with aquatic species generally displaying a fairly small medullary region

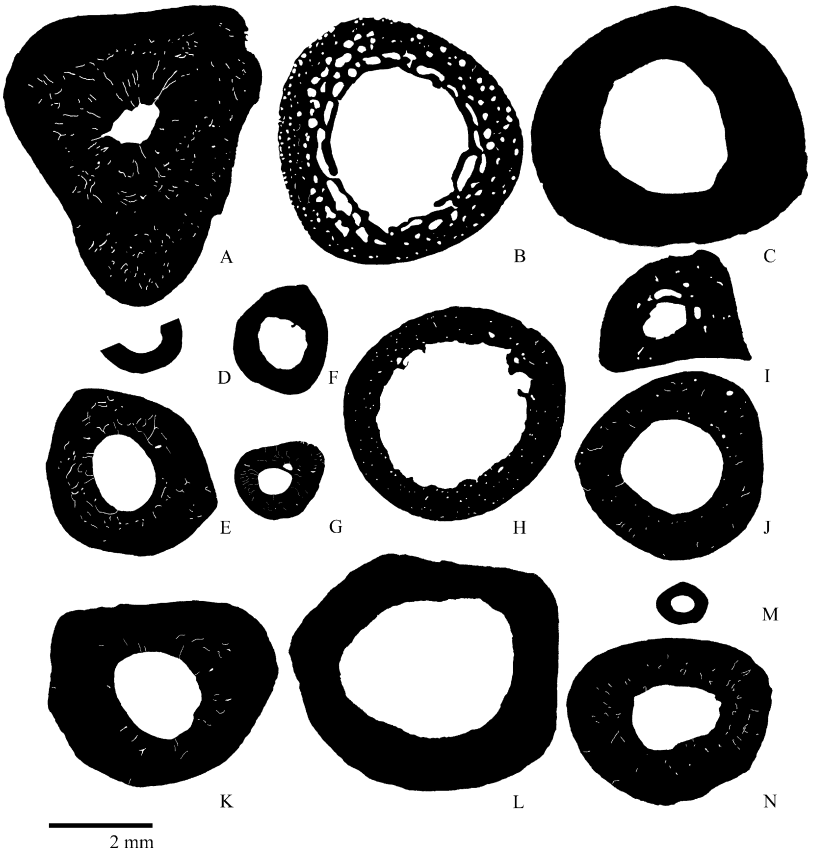


**Fig. 3.** Mid-diaphyseal cross-sections of tibiae of small-sized, aquatic (**A**), amphibious (**B–G**) and terrestrial (**H–N**) mammals. Taxa are arranged according to their lifestyle and phylogenetic affinities. Taxa illustrated are: **(A)** *Ornithorhynchus anatinus;* **(B)** *Amblonyx cinereus;* **(C)** *Martes foina;* **(D)** *Galemys pyrenaicus;* **(E)** *Mustela lutreola;* **(F)** *Mustela vison;* **(G)** *Arvicola sapidus;* **(H)** *Tachyglossus aculeatus;* **(I)** *Zaedyus pichiy;* **(J)** *Martes martes;* **(K)** *Mustela putorius;* **(L)** *Oryctolagus cuniculus;* **(M)** *Arvicola terrestris;* **(N)** *Solenodon paradoxus*. Scale: 2 mm.

**Fig. 3.** Coupes transversales mi-diaphysaires de tibias de mammifères de petite taille, aquatique (**A**), amphibies (**B–G**), terrestres (**H–N**). Les taxons sont disposés selon leur mode de vie et leur ordre dans la phylogénie. Les taxons représentés sont : **(A)** *Ornithorhynchus anatinus* ; **(B)** *Amblonyx cinereus* ; **(C)** *Martes foina* ; **(D)** *Galemys pyrenaicus* ; **(E)** *Mustela lutreola* ; **(F)** *Mustela vison* ; **(G)** *Arvicola sapidus* ; **(H)** *Tachyglossus aculeatus* ; **(I)** *Zaedyus pichiy* ; **(J)** *Martes martes* ; **(K)** *Mustela putorius* ; **(L)** *Oryctolagus cuniculus* ; **(M)** *Arvicola terrestris* ; **(N)** *Solenodon paradoxus*. Échelle : 2 mm.

(Fig. 1A, C, S) that may be occupied, in cryptobranchids, by a spongiosa (Fig. 1R, S). However, some exceptions occur. For instance, the tibiae of *Proteus anguineus* and *Amphiuma means* (Fig. 1D, E) are not especially compact. This is perhaps not surprising given that the lungs of these highly aquatic forms are probably not required to breathe in water, because they can breathe through their gills and skin, and they have a slow metabolism (Gregory, 2003). Thus, the lungs of aquatic lissamphibians can be inflated or deflated to regulate buoyancy contrary to what happens in most aquatic amniotes (turtles being the exception), that depend almost exclusively on lungs for breathing (Jørgensen, 2000). Nevertheless, *Necturus maculosus*, another perennibranchiate form, has a compact tibia (Fig. 1C). Thus, the selective pressure to increase long bone compactness and thus create ballast must be lower in lissamphibians than in amniotes, and may explain the apparently weaker ecological signal in the long limb bones of amphibians (Canoville and Laurin, 2009; Laurin et al., 2004; Laurin et al., 2009). The tibia of *Ambystoma mexicanum* (Fig. 1B) also displays a low compactness, but this may result from its subadult status; it was excluded from our quantitative analyses for that reason (Kriloff et al., 2008). The tibia of *Amphiuma means* (Fig. 1E) shows a fairly thin cortex, but this large amphibian has such diminutive limbs that long bone density in that form must be selectively neutral.

Our sample of amphibious urodeles is too small to draw firm conclusions, but the tibiae do not appear very compact in most cases (Fig. 1F, H). Only *Triturus cristatus* (Fig. 1G) shows what appears to be slight compaction, compared to terrestrial species of salamandrids *Salamandra lanzai, S. atra*, and *S. salamandra* (Fig. 1L–N). This is congruent with the suggestion that globally, there is no difference in compactness between amphibious and terrestrial lissamphibians (Laurin et al., 2004).

Urodele tibiae usually have a very simple, avascular structure (or nearly so; one or two canals are visible in some sections) lacking spongy bone. This probably results partly from their small size, as shown by the fact that the largest urodeles, cryptobranchids, are the only ones to possess spongy bone or medullary resorption cavities (Fig. 1R, S). Another possible explanatory factor is their low metabolic rate, the lowest among tetrapods (Gregory, 2003) and cor-

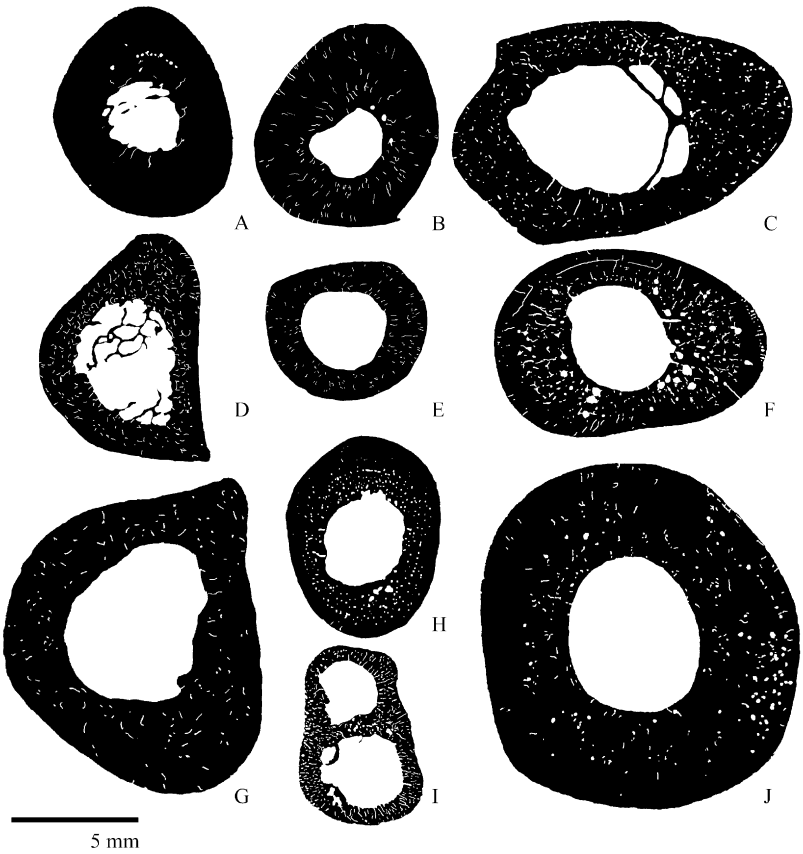


**Fig. 4.** Mid-diaphyseal cross-sections of tibiae of medium-sized, amphibious (**A–B**) and terrestrial (**C–J**) mammals. Taxa are arranged according to their lifestyle and phylogenetic affinities. Taxa illustrated are: **(A)** *Lutra lutra;* **(B)** *Myocastor coypus;* **(C)** *Hystrix cristata;* **(D)** *Cuniculus paca;* **(E)** *Dasyprocta* sp.; **(F)** *Chlorocebus aethiops;* **(G)** *Hylobates* sp.; **(H)** *Macaca radiata;* **(I)** *Erinaceus europaeus;* **(J)** *Capreolus capreolus*. Scale: 5 mm.

**Fig. 4.** Coupes transversales mi-diaphysaires de tibias de mammifères de taille moyenne, amphibies (**A–B**), terrestres (**C–J**). Les taxons sont disposés selon leur mode de vie et leur ordre dans la phylogénie. Les taxons représentés sont : **(A)** *Lutra lutra* ; **(B)** *Myocastor coypus* ; **(C)** *Hystrix cristata* ; **(D)** *Cuniculus paca* ; **(E)** *Dasyprocta* sp. ; **(F)** *Chlorocebus aethiops* ; **(G)** *Hylobates* sp. ; **(H)** *Macaca radiata* ; **(I)** *Erinaceus europaeus* ; **(J)** *Capreolus capreolus*. Échelle : 5 mm.

related low activity level, because anurans display a slightly more complex structure, with at least more vascularization in the largest forms (Figs. 1T, 2).

The tibiofibula of anurans reaches a greater diameter than the tibia of urodeles (Fig. 2). This presumably reflects the important role that the hindlimb plays in anuran locomotion, whereas the largest urodeles (cryptobranchids, amphiumids, sirenids, etc.) are all aquatic forms whose main locomotor structure is presumably the tail, and even terrestrial urodeles have smaller limbs, compared to their body size, than anurans. In a few cases (Fig. 2F), the medullary cavity appears to be subdivided in two, which may represent incomplete integration between fused tibia and fibula, but in most cases, no such subdivision is visible. As for urodeles, lifestyle-dependent patterns in tibial microanatomy are rather subtle and subject to exception. Of the four aquatic species shown here, only two (Fig. 2B, L), the pipids *Pipa carvalhoi* and *Xenopus laevis*, exhibit clearly compact and complex cross-sections with resorption spaces. This may reflect the fact that pipids have been aquatic at least since the Cretaceous, whereas *Bombina* and *Telmatobius* (Fig. 2A, K) may have become aquatic much more recently, as suggested by an optimization of lifestyle on a time-calibrated tree of Lissamphibia (Laurin et al., 2009: Fig. 1A).

Amphibious anurans infrequently show increased compactness, as for amphibious urodeles. Of five taxa, only two, *Discoglossus* sp. and *Ascaphus truei* (Fig. 2E, F), have compact tibiae; all other amphibious anurans (Fig. 2C, D, M) display a degree of compactness typical of terrestrial anurans. Furthermore, the great compactness of *Discoglossus* and *Ascaphus* may perhaps represent a primitive condition for Anura, as most basal anurans (often referred to as "paleobatrachids") display great compactness, except for the aquatic *Bombina orientalis* (Fig. 2A). However, most of these are aquatic or amphibious, so discriminating between these two hypotheses (high compactness of basal anurans resulting from their habitat vs. a phylogenetic effect) would require a greater taxonomic sample, especially of terrestrial, basal anurans.

Among small mammals, our sample includes a single aquatic (borderline amphibious) species, the monotreme *Ornithorhynchus anatinus* (Fig. 3A). Its tibia is compact, especially when compared with its terrestrial sister-group, the monotreme *Tachyglossus aculeatus* (Fig. 3H). Amphibious mammals of small size do not appear to have especially

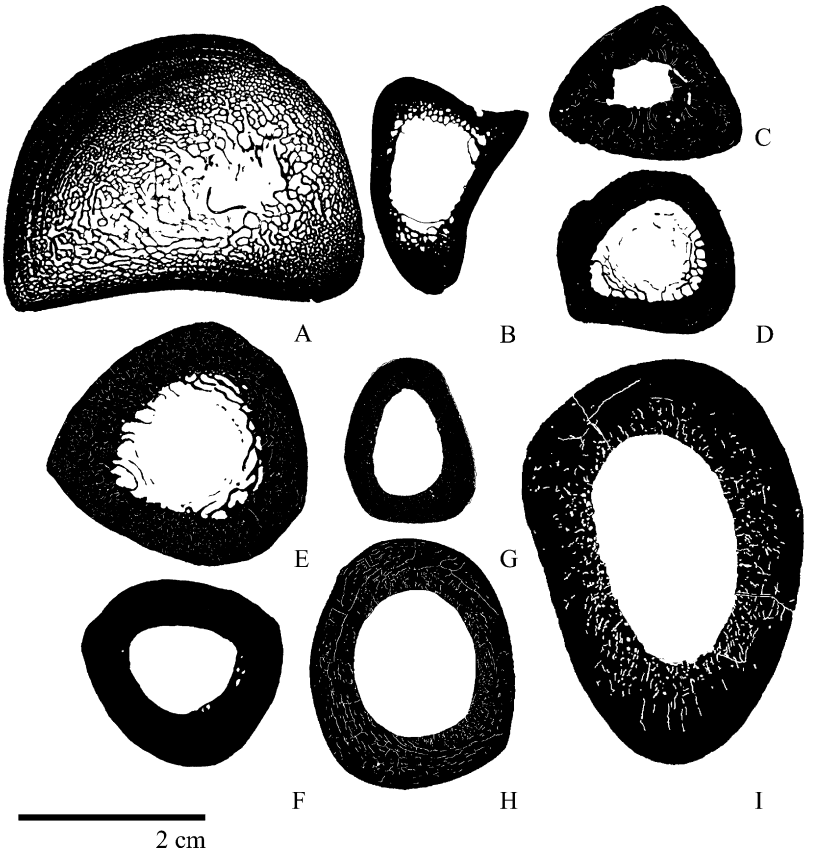


**Fig. 5.** Mid-diaphyseal cross-sections of tibiae of large, aquatic (**A**), amphibious (**B**) and terrestrial (**C–I**) mammals. Taxa are arranged according to their lifestyle and phylogenetic affinities. Taxa illustrated are: **(A)** *Mirounga leonina*; **(B)** *Hydrochoerus hydrochaeris;* **(C)** *Homo sapiens;* **(D)** *Ursus americanus;* **(E)** *Panthera leo;* **(F)** *Canis lupus;* **(G)** *Sus scrofa;* **(H)** *Cervus elaphus;* **(I)** *Camelus dromedarius.* Scale: 2 cm.

**Fig. 5.** Coupes transversales mi-diaphysaires de tibias de mammifères de grande taille, aquatique (**A**), amphibies (**B**), terrestres (**C–I**). Les taxons sont disposés selon leur mode de vie et leur ordre dans la phylogénie. Les taxons représentés sont : **(A)** *Mirounga leonina* ; **(B)** *Hydrochoerus hydrochaeris* ; **(C)** *Homo sapiens* ; **(D)** *Ursus americanus* ; **(E)** *Panthera leo* ; **(F)** *Canis lupus* ; **(G)** *Sus scrofa* ; **(H)** *Cervus elaphus* ; **(I)** *Camelus dromedarius.* Échelle : 2 cm.

compact bone (Fig. 3B–G). The low compactness of the cortex of *Amblonyx cinereus* (Fig. 3B) may possibly result from a subadult, rather than truly adult status; that unnumbered specimen from the comparative anatomy collection of the Muséum National d'Histoire Naturelle, Paris (MNHN) measures only 40 cm in total length (tail included), but adults of the species normally measure over 60 cm (Larivière, 2003). More specimens will be needed to clarify this issue. Even small mammals have tibiae with a complex structure; resorption lacunae, spongy, trabecular bone, and a fairly dense vascular network characterize most tibiae (Fig. 3), even at diameters similar to those of the largest urodele and anuran tibiae (Fig. 1 and 2).

Among mid-sized mammals, our sample includes no aquatic species, and only two amphibious ones, the carnivoran *Lutra lutra* and the rodent *Myocastor coypus* (Fig. 4A, B), but both have more compact tibiae than terrestrial mammals of the same size range (Fig. 4C–J). Unexpectedly, the terrestrial lagomorph *Cuniculus paca* and, to a lesser extent the rodent *Hystrix cristata,* have a few medullary trabeculae (Fig. 4C, D), a feature mostly seen (and usually better developed) in aquatic tetrapods (Figs. 1R, 2B, 5A). Globally, the structure of the tibia of mid-sized mammals (Fig. 4) is more complex than that of small mammals (Fig. 3), with more resorption cavities, more spongiosa and more vascularization. Such structural size effects were already demonstrated by quantitative, statistical studies controlling for phylogenetic effects (Cubo et al., 2005).

The single sampled large aquatic mammal, the phocid *Mirounga leonina* (Fig. 5A) has an extensive spongiosa and a fairly thin cortex that gradually merge into each other, as in Neogene cetacean bones (Canoville and Laurin, 2010; de Buffrénil and Schoevaert, 1988; de Ricqlès and de Buffrénil, 2001). It is thus identifiable as belonging to an aquatic mammal. On the contrary, the single large amphibious mammal, the caviid *Hydrochoerus hydrochaeris* (Fig. 5B), lacks any obvious aquatic adaptation. That may result from the fact that it swims mostly at the surface, a behavior for which increased compactness would be disadvantageous. It has a transitional spongiosa between the cortex and medulla, but so do the terrestrial carnivorans *Ursus americanus* and *Panthera leo* (Fig. 5D, E). The transitional spongiosa of *Ursus* and *Panthera* is not a synapomorphy of these taxa because it is absent in *Canis lupus* (Fig. 5F), which is more closely related to *Ursus* than to *Panthera*. The struc-

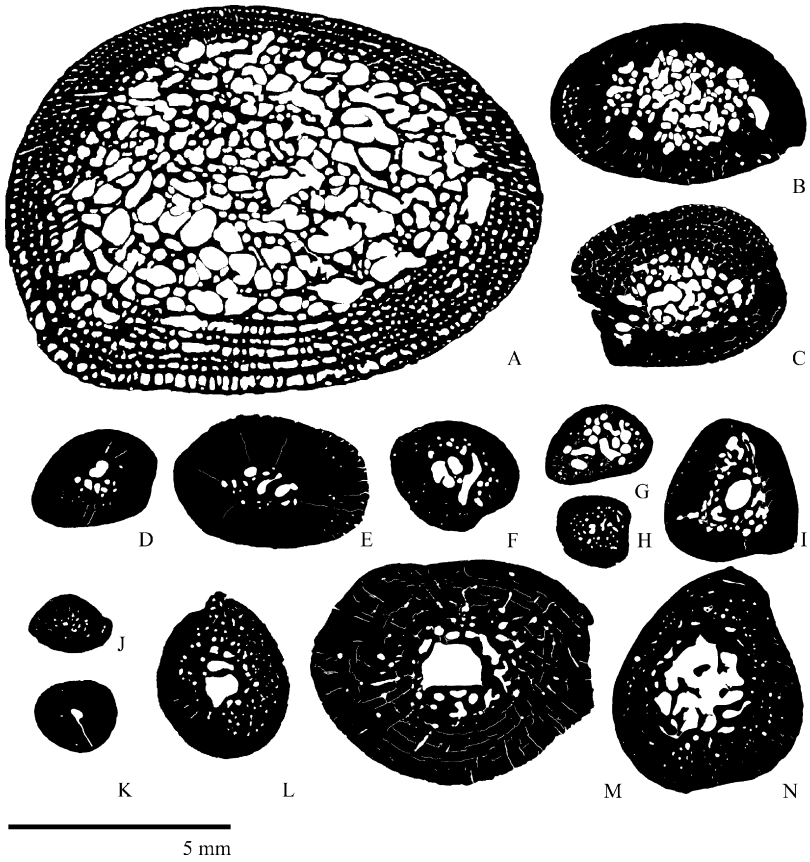


**Fig. 6.** Mid-diaphyseal cross-sections of tibiae of, aquatic (marine **A–B;** freshwater **C–I**) and terrestrial (**J–N**) testudines. Taxa are arranged according to their lifestyle and phylogenetic affinities. Taxa illustrated are: **(A)** *Dermochelys coriacea;* **(B)** *Chelonia mydas;* **(C)** *Chelydra rossignonii*; **(D)** *Pelomedusa subrufa;* **(E)** *Chelus fimbriata;* **(F)** *Malaclemys terrapin;* **(G)** *Emys orbicularis;* **(H)** *Kinosternon;* **(I)** *Pelodiscus sinensis;* **(J)** *Testudo hermanni;* **(K)** *Homopus femoralis;* **(L)** *Testudo graeca;* **(M)** *Astrochelys radiata;* **(N)** *Geochelone carbonaria.* Scale: 5 mm.

**Fig. 6.** Coupes transversales mi-diaphysaires de tibias de tortues, aquatiques (marines **A–B;** d'eau douce **C–I**), et terrestres (**J–N**). Les taxons sont disposés selon leur mode de vie et leur ordre dans la phylogénie. Les taxons représentés sont : **(A)** *Dermochelys coriacea* ; **(B)** *Chelonia mydas* ; **(C)** *Chelydra rossignonii* ; **(D)** *Pelomedusa subrufa* ; **(E)** *Chelus fimbriata* ; **(F)** *Malaclemys terrapin* ; **(G)** *Emys orbicularis* ; **(H)** *Kinosternon* ; **(I)** *Pelodiscus sinensis* ; **(J)** *Testudo hermanni* ; **(K)** *Homopus femoralis* ; **(L)** *Testudo graeca* ; **(M)** *Astrochelys radiata* ; **(N)** *Geochelone carbonaria.* Échelle : 5 mm.

ture of the tibia of large mammals (Fig. 5) is even more complex than that of mid-sized mammals (Fig. 4). Spongy bone and vascularization are especially well-developed.

Chelonians (Testudinata) prove atypical of tetrapods in their relationship between long bone microanatomy and habitat, as has been previously noted (Canoville and Laurin, 2010; Germain and Laurin, 2005; Kriloff et al., 2008). So far, no clear ecological signal has been found in their long bone microanatomy, although ecological indicators of lifestyle appear to be present in the microanatomy and histology of the turtle shell (Scheyer and Sander, 2007). The lack of statistically significant results so far for this taxon alone may result partly from the small taxonomic sample size: seven species for the radius (Germain and Laurin, 2005), fourteen species for the tibia (Kriloff et al., 2008), and thirteen species for the humerus (Canoville and Laurin, 2010). More likely, turtle body density may be adjusted in evolution through changes in the carapace (Kriloff et al., 2008), rather than in long limb bones, and it can be adjusted behaviourally by regulating the lung volume (Jørgensen, 2000: 306). In any case, terrestrial turtles clearly show an anomalous pattern of high compactness and an extensive medullary spongiosa that may nevertheless leave a small medullary cavity (Fig. 6J–N). In Fig. 6, the tibiae of the fourteen species previously studied (Kriloff et al., 2008) are illustrated. One of the two marine turtles, *Dermochelys coriacea* (Fig. 6A) has a much less compact tibia, with a highly porous cortex. However, that tibia is also by far the largest, so this difference may result from a body-size effect or may be a clade effect rather than an ecological difference. All other tibial sections resemble each other in having an extensive spongiosa, even in terrestrial turtles, a rather thick cortex, and various resorption spaces and vascular cavities (Fig. 6).

Among diapsids, subtle habitat-linked differences are noticeable (Fig. 7). Amphibious diapsids tend to have a thicker cortex than terrestrial ones (no section of an extant aquatic diapsid tibia is available in our collection). This thickening of the cortex (along with, in this case, more abundant vascularization) is best visible in *Crocodylus niloticus* (Fig. 7K), although in this case, body size or phylogenetic effects cannot be dismissed because

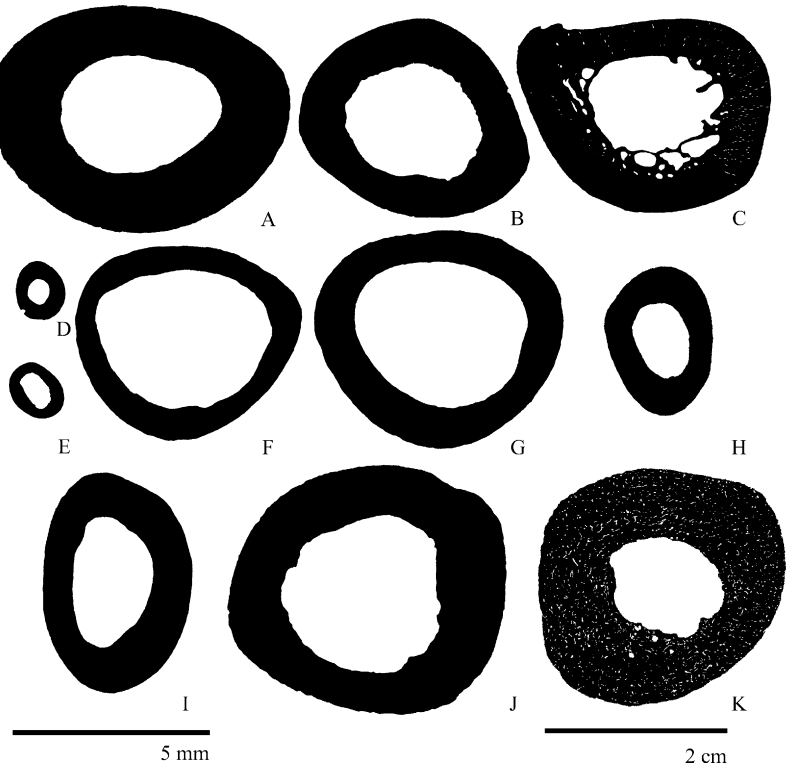


**Fig. 7.** Mid-diaphyseal cross-sections of tibiae of amphibious (**A–C, K**) and terrestrial (**D–J**) diapsids. Taxa are arranged according to their lifestyle and phylogenetic affinities. Taxa illustrated are: **(A)** *Amblyrhynchus cristatus;* **(B)** *Varanus niloticus;* **(C)** *Varanus salvator;* **(D)** *Sceloporus horridus horridus;* **(E)** *Sceloporus oligoporus*; **(F)** *Ctenosaura pectinata;* **(G)** *Iguana iguana;* **(H)** *Uromastyx acanthinurus;* **(I)** *Varanus griseus;* **(J)** *Varanus komodoensis* (juvenile); **(K)** *Crocodylus niloticus.* Scale: (**A–J**): 5 mm; (**K**): 2 cm.

**Fig. 7.** Coupes transversales mi-diaphysaires de tibias de diapsides amphibies (**A–C, K**) et terrestres (**D–J**). Les taxons sont disposés selon leur mode de vie et leur ordre dans la phylogénie. Les taxons représentés sont : **(A)** *Amblyrhynchus cristatus* ; **(B)** *Varanus niloticus* ; **(C)** *Varanus salvator* ; **(D)** *Sceloporus horridus horridus* ; **(E)** *Sceloporus oligoporus* ; **(F)** *Ctenosaura pectinata* ; **(G)** *Iguana iguana* ; **(H)** *Uromastyx acanthinurus* ; **(I)** *Varanus griseus* ; **(J)** *Varanus komodoensis* (juvénile) ; **(K)** *Crocodylus niloticus.* Échelle : (**A–J**) : 5 mm; (**K**) : 2 cm.

that tibia is by far the largest in our sample, and it is the only crocodylian studied. More moderate thickening is also visible in *Amblyrhynchus cristatus* (Fig. 7A), the marine iguana from the Galapagos Islands, especially if contrasted with its sister-group in the sample, *Iguana iguana* (Fig. 7G). Among the two amphibious *Varanus* taxa included, only *Varanus salvator* (Fig. 7C) differs from terrestrial members of *Varanus* in displaying a more complex structure with resorption spaces and a transitional spongiosa; our sample size is insufficient to determine if such a spongiosa frequently occurs in amphibious diapsid tibiae, although it is known to occur in the humerus and other bones of several aquatic diapsids, such as plesiosaurs and ichthyosaurs (Canoville and Laurin, 2010; de Buffrénil and Mazin, 1990; de Buffrénil and Mazin, 1993; de Buffrénil et al., 1987; Wiffen et al., 1995). *V. niloticus* (Fig. 7B) does not appear very different from the terrestrial *V. griseus* and *V. komodoensis* (Fig. 7I, J). However, the comparison with *V. komodoensis* is tentative because the sectioned specimen is juvenile, as indicated by its relatively small size.

## 4. Structure and functional interpretation of tetrapod long bones: radius

So far, we investigated the radius only among amniotes. The radius of small amphibious mammals (Fig. 8A–H) tends to be more compact than that of terrestrial mammals (Fig. 8I–X). This is especially obvious for the monotreme *Ornithorhynchus anatinus,* the carnivoran *Mustela lutreola,* and the rodents *Ondatra zybethicus, Castor canadensis,* and *Myocastor coypus* (Fig. 8A, C, F–H). The radius of the carnivoran *Amblonyx cinereus* does not appear particularly compact, but as mentioned above, it may be a juvenile specimen. The cortex of the radius of primates looks porous (Fig. 8V–X), especially in *Chlorocebus aethiops* (Fig. 8W). This probably does not reflect their arborical lifestyle because the tibial cortex of primates is more compact (Fig. 4) and the radius of the rodent *Hystrix cristata* (Fig. 8S), that often climbs trees (M. L., personal observation) is fairly compact.

Our sample includes only three radii of mid–sized mammals, one amphibious (Fig. 9A) and two terrestrial ones (Fig. 9B–C). As for the tibia, the radius of *Hydrochoerus hydrochaeris* features a transitional spongiosa (Fig. 9A), but it does not differ otherwise from the radius of similar-sized terrestrial mammals, such as *Canis lupus* or the cervid *Capreolus capreolus* (Fig. 9B–C). Among large mammals, the difference between aquatic and terrestrial taxa is striking. Aquatic forms (Fig. 9D–G) have an extensive spongiosa that either occupies all of the medullary region, as in the pinnipeds *Otaria byronia* and *Arctocephalus australis* or in the cetacean *Phocoena phocoena* (Fig. 9D–F), or that grades gen-

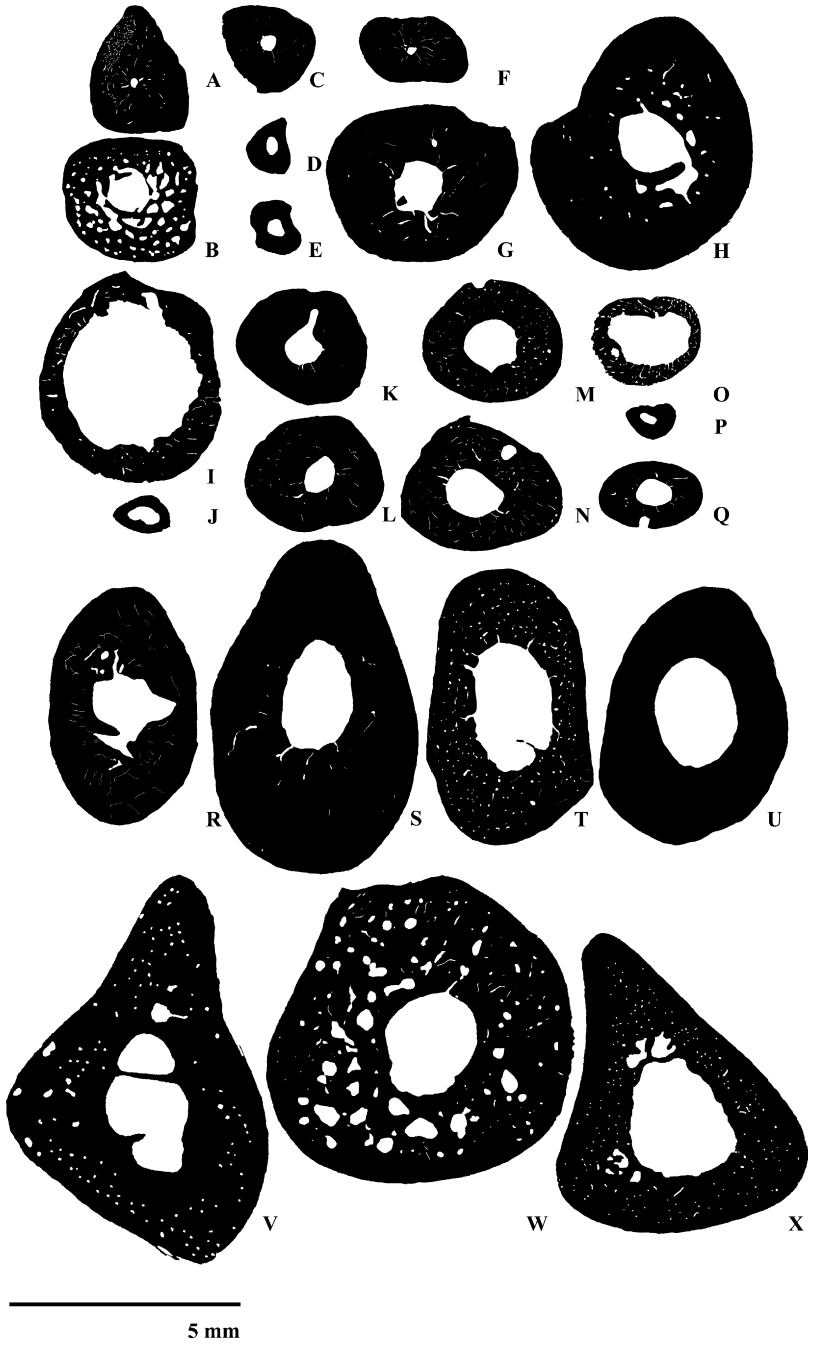


**Fig. 8.** Mid-diaphyseal cross-sections of radii of small amphibious (**A–H**) and terrestrial (**I–X**) mammals. Taxa are arranged according to their lifestyle and phylogenetic affinities. Taxa illustrated are: **(A)** *Ornithorhynchus anatinus;* **(B)** *Amblonyx cinereus;* **(C)** *Mustela lutreola*; **(D)** *Galemys pyrenaicus;* **(E)** *Arvicola zapidus;* **(F)** *Ondatra zybethicus;* **(G)** *Castor canadensis;* **(H)** *Myocastor coypus;* **(I)** *Tachyglossus oculeata;* **(J)** *Mustela nivalis;* **(K)** *Mustela vison;* **(L)** *Mustela putorius;* **(M)** *Martes martes;* **(N)** *Martes foina;* **(O)** *Erinaceus europaeus;* **(P)** *Arvicola terrestris;* **(Q)** *Cavia porcellus;* **(R)** *Marmota marmota;* **(S)** *Hystrix cristata;* **(T)** *Cuniculus paca;* **(U)** *Dasyprocta agouti;* **(V)** *Hylobates* sp.; **(W)** *Chlorocebus aethiops;* **(X)** *Macaca radiata.* Scale: 5 mm.

**Fig. 8.** Coupes transversales mi-diaphysaires de radius de mammifères de petite taille, amphibies (**A–H**) et terrestres (**I–X**). Les taxons sont disposés selon leur mode de vie et leur ordre dans la phylogénie. Les taxons représentés sont : **(A)** *Ornithorhynchus anatinus* ; **(B)** *Amblonyx cinereus* ; **(C)** *Mustela lutreola* ; **(D)** *Galemys pyrenaicus* ; **(E)** *Arvicola zapidus* ; **(F)** *Ondatra zybethicus* ; **(G)** *Castor canadensis* ; **(H)** *Myocastor coypus* ; **(I)** *Tachyglossus oculeata* ; **(J)** *Mustela nivalis* ; **(K)** *Mustela vison* ; **(L)** *Mustela putorius* ; **(M)** *Martes martes* ; **(N)** *Martes foina* ; **(O)** *Erinaceus europaeus* ; **(P)** *Arvicola terrestris* ; **(Q)** *Cavia porcellus* ; **(R)** *Marmota marmota* ; **(S)** *Hystrix cristata* ; **(T)** *Cuniculus paca* ; **(U)** *Dasyprocta agouti* ; **(V)** *Hylobates* sp. ; **(W)** *Chlorocebus aethiops* ; **(X)** *Macaca radiata.* Échelle : 5 mm.

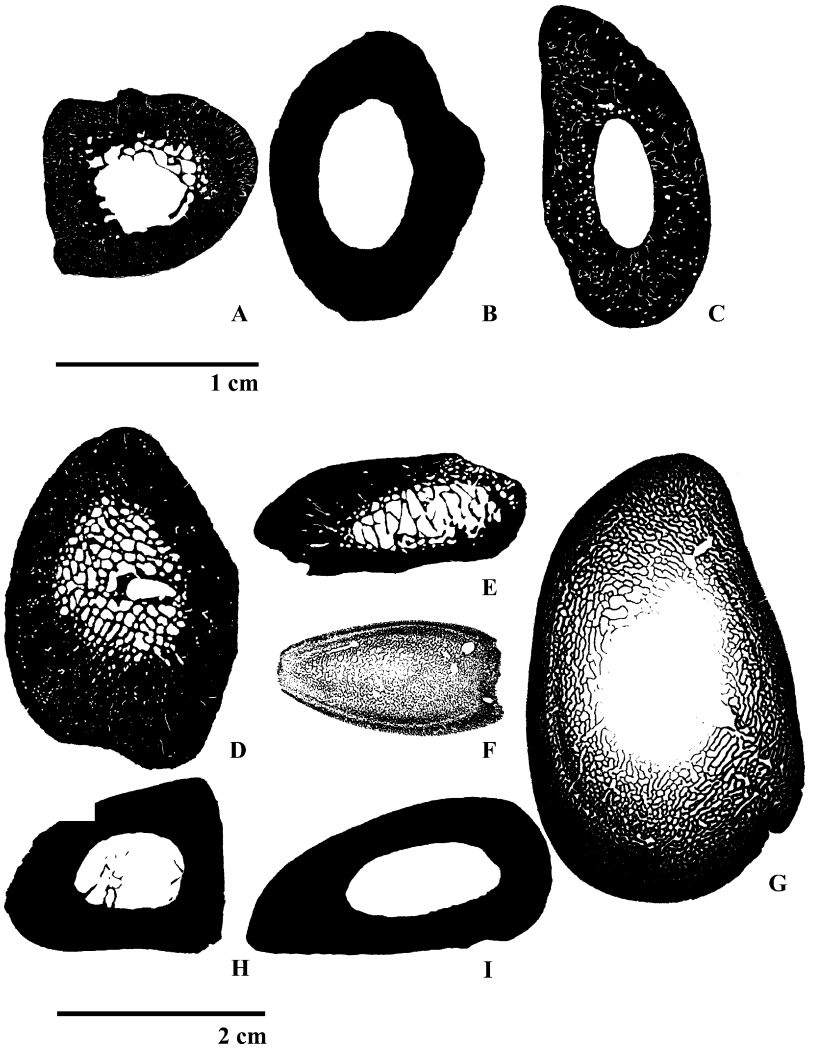


**Fig. 9.** Mid-diaphyseal cross-sections of radii of mid-sized (**A–C**) and large (**D–I**) mammals, of aquatic (**D–G**), amphibious (**A**) and terrestrial (**B–C**, **H–I**) lifestyle. Taxa are arranged according to their lifestyle and phylogenetic affinities. Taxa illustrated are: **(A)** *Hydrochoerus hydrochaeris;* **(B)** *Canis lupus;* **(C)** *Capreolus capreolus*; **(D)** *Otaria byronia*; **(E)** *Arctocephalus australis*; **(F)** *Phocoena phocoena;* **(G)** *Mirounga leonina;* **(H)** *Ursus americanus;* **(I)** *Cervus elaphus.* Scale: (**A–C**):1 cm; (**D–I**): 2 cm.

**Fig. 9.** Coupes transversales mi-diaphysaires de radius de mammifères placentaires de moyenne (**A–C**) et grande (**D–I**) taille, aquatiques (**D–G**), amphibies (**A**) et terrestres (**B–C**, **H–I**). Les taxons sont disposés selon leur mode de vie et leur ordre dans la phylogénie. Les taxons représentés sont : **(A)** *Hydrochoerus hydrochaeris* ; **(B)** *Canis lupus* ; **(C)** *Capreolus capreolus* ; **(D)** *Otaria byronia* ; **(E)** *Arctocephalus australis* ; **(F)** *Phocoena phocoena* ; **(G)** *Mirounga leonina* ; **(H)** *Ursus americanus* ; **(I)** *Cervus elaphus.* Échelle : (**A–C**) : 1 cm; (**D–I**) : 2 cm.

tly into the medullary region, as in the phocid *Mirounga leonina* (Fig. 9G). The two mammalian terrestrial taxa in that size range (*Ursus americanus* and *Cervus elaphus*) have very distinct, typically terrestrial radii with a moderately thick, compact cortex, and virtually no trabecular bone in the mid-diaphyseal area (Fig. 9H–I).

The radius of mid-sized turtles (Fig. 10A–F) shows no obvious difference between amphibious (Fig. 10A–C) and terrestrial (Fig. 10D–F) taxa. Among the latter, *Testudo graeca* (Fig. 10E) has an extensive spongiosa and looks very similar to amphibious turtles. However, the two other terrestrial turtles, *Geochelone carbonaria* and *Homopus femoralis* (Fig. 10D, F) show a thick, compact cortex and no spongiosa, which is atypical of turtle long bones. It is tempting to suggest a link with their terrestrial lifestyle, but among the tibiae sectioned, only *Homopus femoralis* (Fig. 6K) shows the same pattern. Other terrestrial turtles (i.e. tortoises) show a variably–developed spongiosa; this includes *Testudo hermanni, Testudo graeca, Astrochelys radiata,* and *Geochelone carbonaria* (Fig. 6J, L–N). As for the tibia, the radius of the sampled marine turtle *Chelonia mydas* differs by its more complex structure, with a more porous cortex and a well-developed medullary spongiosa (Fig. 10G). Again, because of sample size limitation, it is not clear if this is a simple body size effect, or if this reflects the pelagic lifestyle of *C. mydas*.

The sample size of the radius of diapsids is too small to allow definitive statements about habitat-related compactness patterns. Nevertheless, the single amphibious squamate, *Amblyrhynchus cristatus,* has a much more com-

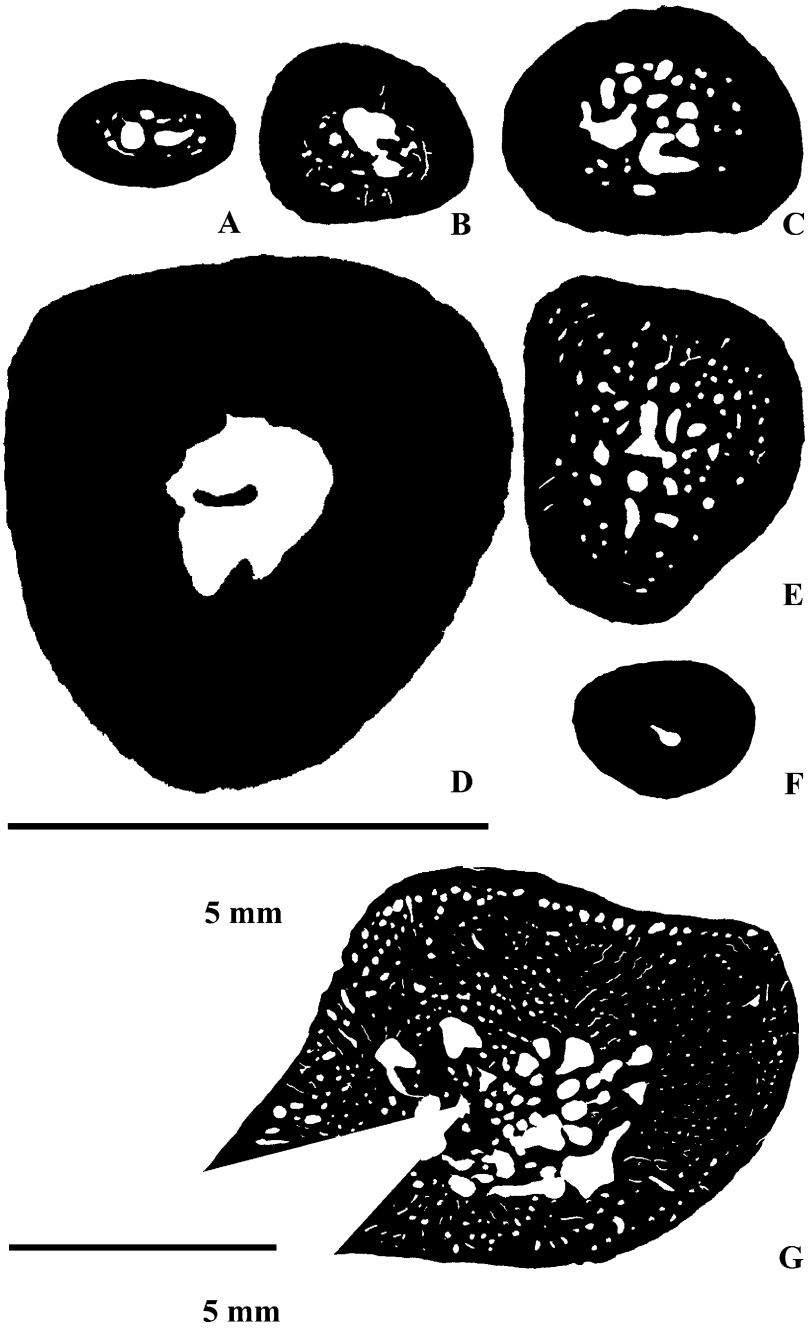


**Fig. 10.** Mid-diaphyseal cross-sections of radii of mid-sized (**A–F**) and large (**G**) testudines of aquatic (**G**), amphibious (**A–C**), and terrestrial (**D–F**) lifestyle. Taxa are arranged according to their lifestyle and phylogenetic affinities. Taxa illustrated are: **(A)** *Emys orbicularis*; **(B)** *Pelodiscus sinensis;* **(C)** *Chelus fimbriata;* **(D)** *Geochelone carbonaria*; **(E)** *Testudo graeca;* **(F)** *Homopus femoralis;* **(G)** *Chelonia mydas.* Scale: 5 mm.

**Fig. 10.** Coupes transversales mi-diaphysaires de radius de tortues de moyennes (**A–F**) et grandes (**G**) tailles et de mode de vie aquatique (**G**), amphibie (**A–C**) et terrestre (**D–F**). Les taxons sont disposés selon leur mode de vie et leur ordre dans la phylogénie. Les taxons représentés sont : **(A)** *Emys orbicularis* ; **(B)** *Pelodiscus sinensis* ; **(C)** *Chelus fimbriata* ; **(D)** *Geochelone carbonaria* ; **(E)** *Testudo graeca* ; **(F)** *Homopus femoralis* ; **(G)** *Chelonia mydas.* Échelle : 5 mm.

pact radius than its sister-group, *Iguana iguana* (Fig. 11E, F), as noted above for the tibia. The radius of *Crocodylus niloticus* resembles the tibia in its small medullary cavity and the extensive vascularization in the cortex (Fig. 11I). All other sampled diapsids are terrestrial squamates; these all have a compact, avascular cortex and lack trabeculae. No size-related differences are detectable.

## 5. Structure and functional interpretation of tetrapod long bones: humerus

The humerus has been investigated in both lissamphibians and amniotes, but only the latter will be described here because the drawings of lissamphibian humeri are already published (Canoville and Laurin, 2009). In small mammals,

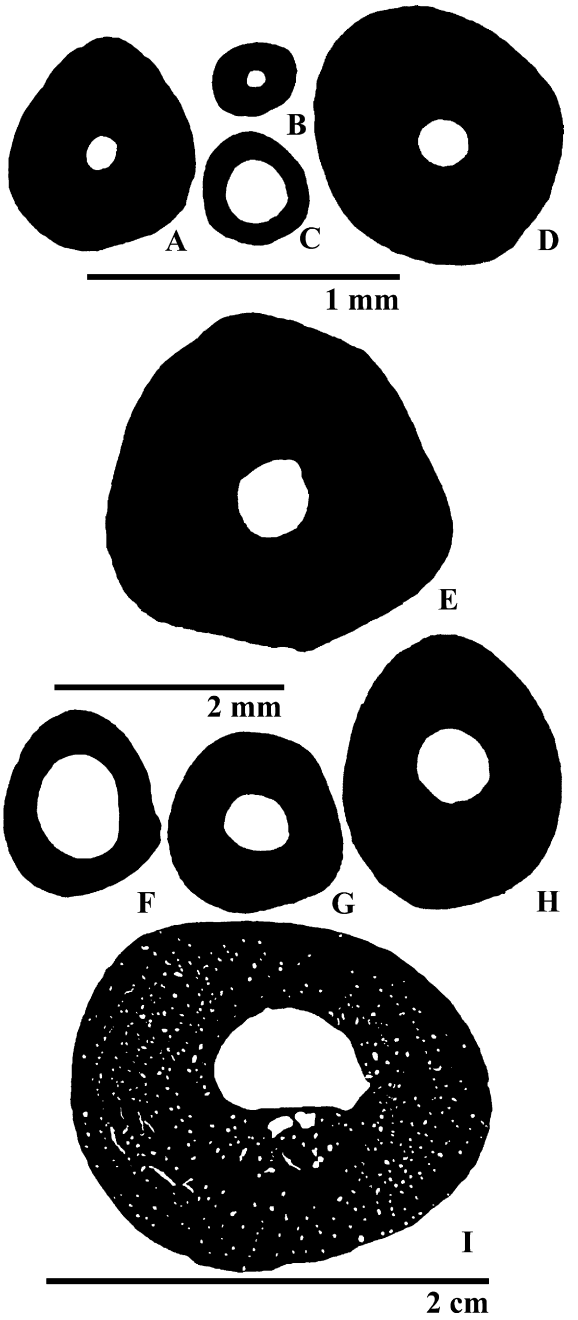


**Fig. 11.** Drawings of mid-diaphyseal cross-sections of radii of diapsids of small (**A–D**), medium (**E–H**), and large (**I**) body size (maximal diameter from 0.28 mm to 19.26 mm) and of amphibious (**E, I**) and terrestrial (**A–D, F–H**) lifestyle. Taxa are arranged according to their lifestyle and phylogenetic affinities. Taxa illustrated are: **(A)** *Sceloporus horridus;* **(B)** *Urosaurus bicarinatus;* **(C)** *Cnemidophorus deppei;* **(D)** *Gerrhonotus viridiflavana;* **(E)** *Amblyrhynchus cristatus;* **(F)** *Iguana iguana;* **(G)** *Uromastyx acanthinura;* **(H)** *Varanus griseus;* **(I)** *Crocodylus niloticus.* Scale: (**A–D**): 1 mm; (**E–H**): 2 mm; (**I**): 2 cm.

**Fig. 11.** Coupes transversales mi-diaphysaires de radius de diapsides de petite (**A–D**), moyenne (**E–H**) et grande (**I**) tailles (diamètre maximal des sections de 0,28 mm à 19,26 mm) et de mode de vie amphibie (**E, I**) et terrestre (**A–D, F–H**). Les taxons sont disposés selon leur mode de vie et leur ordre dans la phylogénie. Les taxons représentés sont : **(A)** *Sceloporus horridus* ; **(B)** *Urosaurus bicarinatus* ; **(C)** *Cnemidophorus deppei* ; **(D)** *Gerrhonotus viridiflavana* ; **(E)** *Amblyrhynchus cristatus* ; **(F)** *Iguana iguana* ; **(G)** *Uromastyx acanthinura* ; **(H)** *Varanus griseus* ; **(I)** *Crocodylus niloticus.* Échelles : (**A–D**) : 1 mm; (**E–H**) : 2 mm; (**I**) : 2 cm.

the sampled aquatic species, *Ornithorhynchus anatinus*, has the most compact humerus (Fig. 12A), followed by two of the five sampled amphibious species (*Myocastor coypus* and *Castor canadensis*). The humerus of three amphibious species (the arvicolid *Ondatra zybethicus,* the talpid *Galemys pyrenaicus,* and the mustelid *Amblonyx cinereus*) does not appear particularly compact. Among the terrestrial sample, a single species, the dasypodid *Zaedyus pichiy,* has a com-

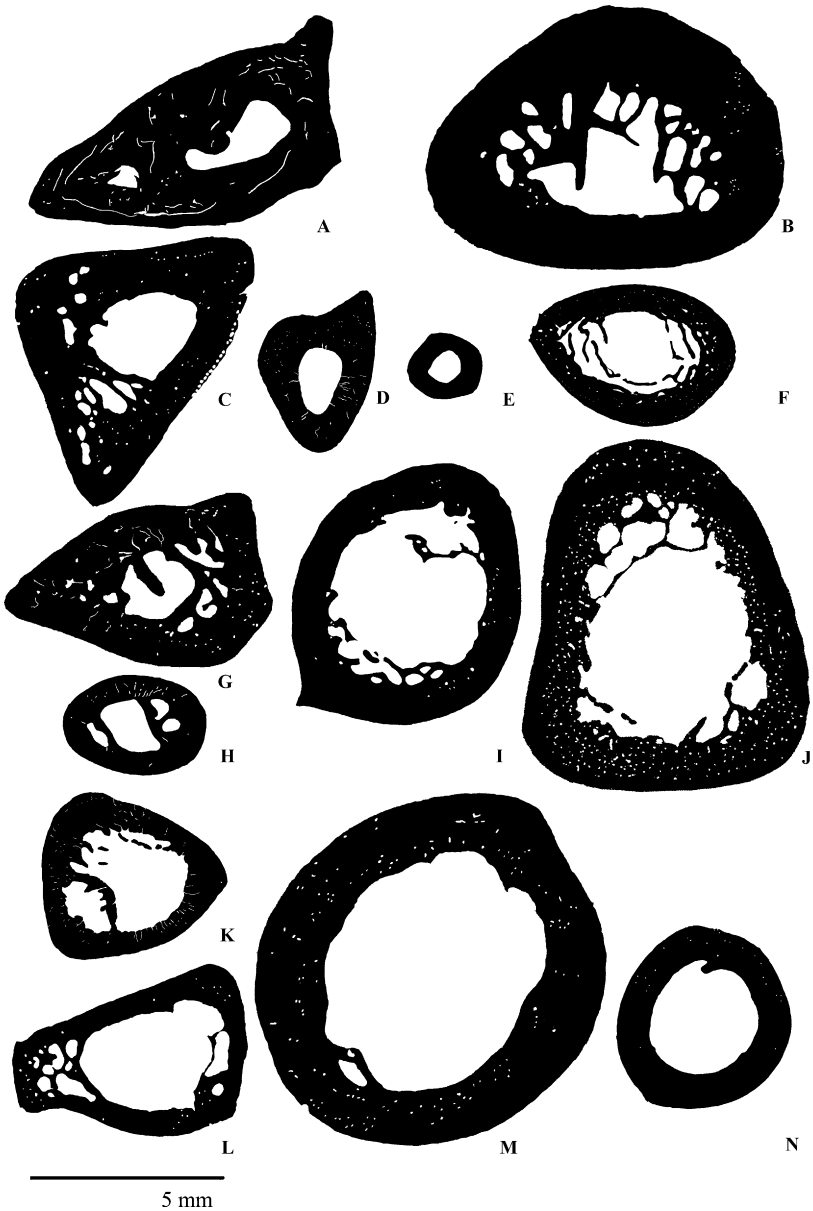


**Fig. 12.** Mid-diaphyseal cross-sections of humeri of medium-sized, aquatic (**A**), amphibious (**B–F**), and terrestrial (**G–N**) mammals. Taxa are arranged according to their lifestyle and phylogenetic affinities. Taxa illustrated are: **(A)** *Ornithorhynchus anatinus*; **(B)** *Myocastor coypus*; **(C)** *Castor canadensis*; **(D)** *Ondatra zybethicus*; **(E)** *Galemys pyrenaicus*; **(F)** *Amblonyx cinereus*; **(G)** *Zaedyus pichyi*; **(H)** *Cavia porcellus*; **(I)** *Marmota marmota*; **(J)** *Macaca radiata*; **(K)** *Erinaceus europaeus*; **(L)** *Solenodon paradoxus*; **(M)** *Vulpes vulpes*; **(N)** *Martes martes*. Scale: 5 mm.

**Fig. 12.** Coupes transversales mi-diaphysaires d'humérus de mammifères de taille moyenne, aquatique (**A**), amphibies (**B–F**) et terrestres (**G–N**). Les taxons sont disposés selon leur mode de vie et leur ordre dans la phylogénie. Les taxons représentés sont : **(A)** *Ornithorhynchus anatinus* ; **(B)** *Myocastor coypus* ; **(C)** *Castor canadensis* ; **(D)** *Ondatra zybethicus* ; **(E)** *Galemys pyrenaicus* ; **(F)** *Amblonyx cinereus* ; **(G)** *Zaedyus pichyi* ; **(H)** *Cavia porcellus* ; **(I)** *Marmota marmota* ; **(J)** *Macaca radiata* ; **(K)** *Erinaceus europaeus* ; **(L)** *Solenodon paradoxus* ; **(M)** *Vulpes vulpes* ; **(N)** *Martes martes*. Échelle : 5 mm.

pact humerus and thick bony trabeculae that partly occlude the medullary cavity. These features, otherwise more typical of aquatic or amphibious mammals, are perhaps linked to its partly fossorial lifestyle (Fig. 12G). All other terrestrial mammals of small size have a fairly thin cortex and little or no spongiosa (Fig. 12 H–N).

Among large mammals, aquatic taxa such as *Dugong dugon*, *Arctocephalus australis* (Fig. 13A, B), and an unidentified species of Miocene dolphin from the Chesapeake Group, USA (Fig. 14A) have much more compact humeri than amphibious or terrestrial species. Pelagic mammals, such as extant cetaceans (Fig. 14 B, C) and a Miocene cetotheriid (Fig. 15C), do not have especially compact bones, but have an extensive spongiosa that fills the medullary region. Pinnipeds usually have an extensive spongiosa (Fig. 15A, B), and their compactness is highly variable, ranging from moderate (Fig. 13B; 15A) to low (Fig. 15B). Mid-sized to large amphibious mammals, such

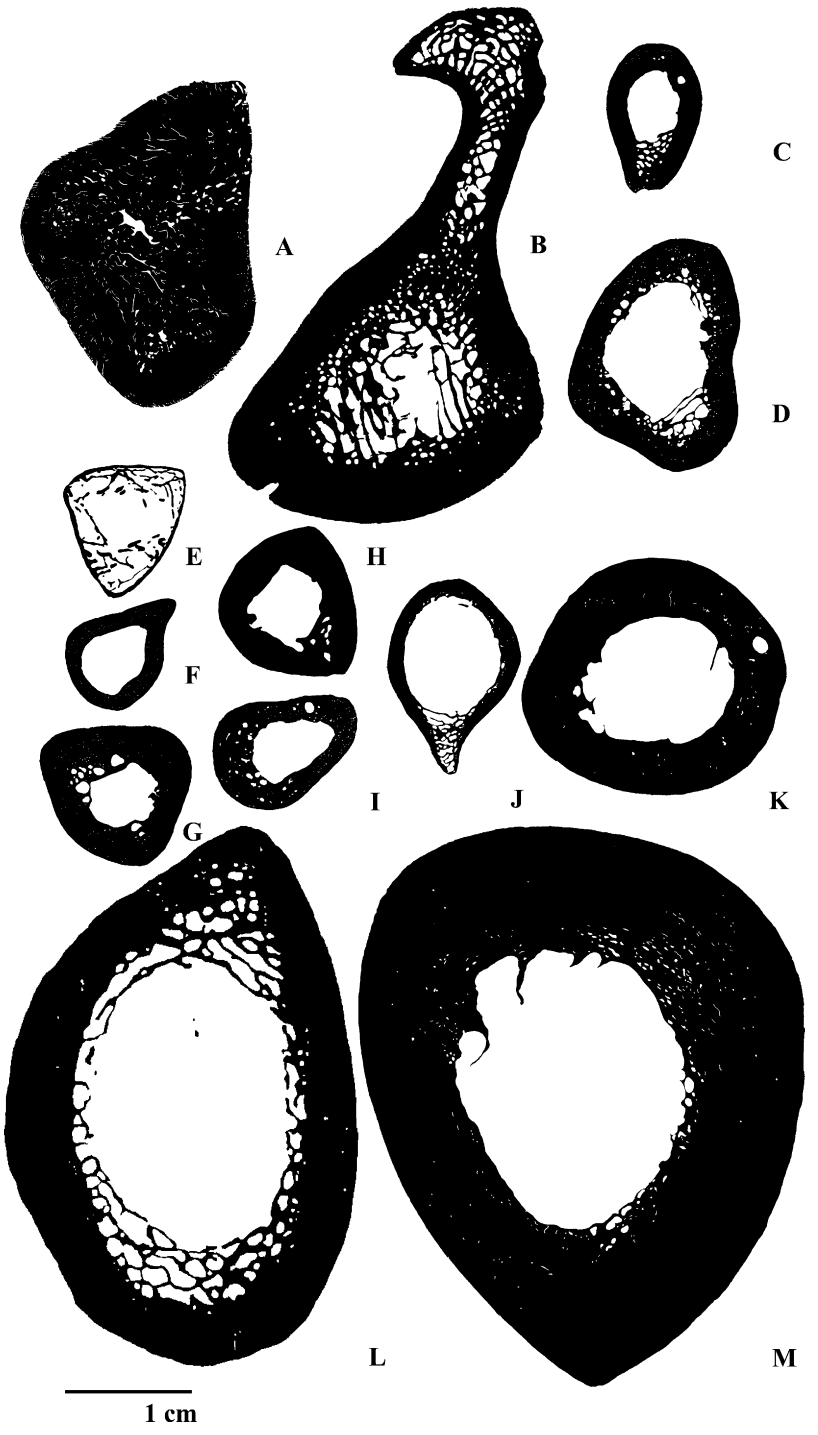


**Fig. 13.** Mid-diaphyseal cross-sections of humeri of large aquatic (**A–B**), amphibious (**C–D**), and terrestrial (**E–M**) mammals. Taxa are arranged according to their lifestyle and phylogenetic affinities. Taxa illustrated are : **(A)** *Dugong dugon*; **(B)** *Arctocephalus australis*; **(C)** *Lutra lutra*; **(D)** *Hydrochoerus hydrochaeris*; **(E)** *Tachyglossus aculeatus*; **(F–G)** *Macropus rufogriseus*; **(H)** *Hystrix cristata*; **(I)** *Chlorocebus aethiops*; **(J)** *Meles meles*; **(K)** *Canis lupus*; **(L)** *Panthera leo*; **(M)** *Equus burchelli*. Scale : 1 cm.

**Fig. 13.** Coupes transversales mi-diaphysaires d'humérus de mammifères aquatiques (**A–B**), amphibies (**C–D**) et terrestres (**E–M**) de grande taille. Les taxons sont disposés selon leur mode de vie et leur ordre dans la phylogénie. Les taxons représentés sont : **(A)** *Dugong dugon*; **(B)** *Arctocephalus australis* ; **(C)** *Lutra lutra* ; **(D)** *Hydrochoerus hydrochaeris* ; **(E)** *Tachyglossus aculeatus* ; **(F–G)** *Macropus rufogriseus* ; **(H)** *Hystrix cristata* ; **(I)** *Chlorocebus aethiops* ; **(J)** *Meles meles* ; **(K)** *Canis lupus* ; **(L)** *Panthera leo* ; **(M)** *Equus burchelli*. Échelle : 1 cm.

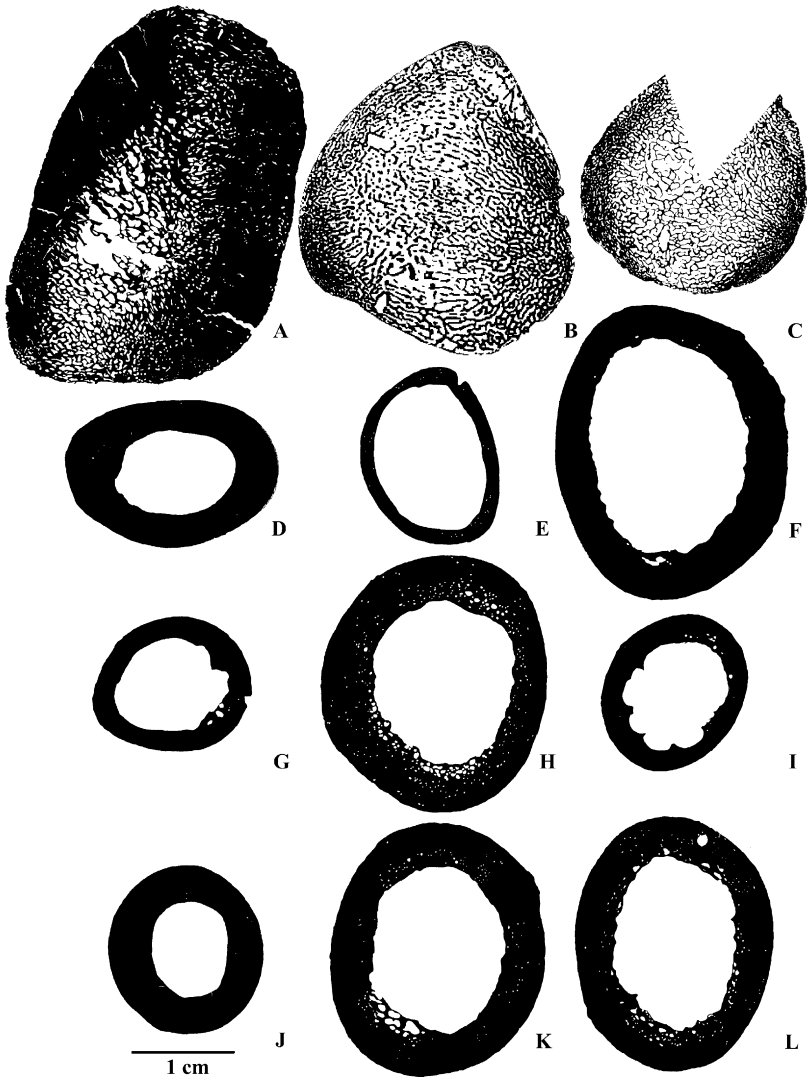


**Fig. 14.** Mid-diaphyseal cross-sections of humeri of large aquatic (**A–C**) and terrestrial (**D–L**) cetartiodactyls. Taxa are arranged according to their lifestyle and phylogenetic affinities. Taxa shown are: **(A)** Delphinidae (Miocene, Chesapeake Group, U.S.A.); **(B)** *Delphinus delphis*; **(C)** *Phocoena phocoena;* **(D)** *Sus scrofa*; **(E)** *Capra hircus*; **(F)** *Capra falconeri*; **(G)** *Ovis ammon*; **(H)** *Ammotragus lervia*; **(I)** *Antilope cervicapra*, **(J)** *Redunca fulvorufula*; **(K–L)** *Kobus leche*. Scale: 1 cm.

**Fig. 14.** Coupes transversales mi-diaphysaires d'humérus de cétartiodactyles de grande taille et de mode de vie aquatique (**A–C**) ou terrestre (**D–L**). Les taxons sont disposés selon leur mode de vie et leur ordre dans la phylogénie. Les taxons représentés sont : **(A)** Delphinidae (Miocene, Chesapeake Group, U.S.A.) ; **(B)** *Delphinus delphis* ; **(C)** *Phocoena phocoena* ; **(D)** *Sus scrofa* ; **(E)** *Capra hircus* ; **(F)** *Capra falconeri* ; **(G)** *Ovis ammon* ; **(H)** *Ammotragus lervia* ; **(I)** *Antilope cervicapra* ; **(J)** *Redunca fulvorufula* ; **(K–L)** *Kobus leche*. Échelle : 1 cm.

as the freshwater otter (*Lutra lutra*) or the capybara (*Hydrochoerus hydrochaeris*) do not have especially compact humeri, and their spongiosa is moderately developed (Fig. 13C, D). Similarly, most terrestrial species have moderately thick, compact cortices with little or no spongiosa, although a few species stand out. The monotreme *Tachyglossus aculeatus* (Fig. 13E) has a very thin cortex with a well-developed transitional spongiosa composed of several fine trabeculae. The placental *Capra hircus* also has a thin cortex, but no spongiosa (Fig. 14E). At the other extreme, the marsupial *Macropus rufogriseus* (red-necked wallaby; Fig. 13G), the zebra *Equus burchelli* (Fig. 13M), and the ruminants *Boselaphus tragocamelus* (Fig. 16B) and *Syncerus caffer* (Fig. 16H) have rather thick, compact cortices. The ruminant *Taurotragus oryx* (Fig. 16A) also has a thick cortex, but it has relatively low compactness. Except for the wallaby, it is tempting to attribute the cortical thickness to the great size of these extant placentals, but the relatively thin cortex of both extant species of bison (Fig. 15D–F) tends to refute this idea. Unfortunately, graviportal mammals are poorly represented in our sample because of difficulty in securing bones for sectioning, but previous studies have shown that graviportal mammals have compact bones. This has been shown for the ribs of the Indonesian rhinoceros (*Rhinoceros sondaicus*) and for limb bones of the large extinct marsupials *Zygo-*

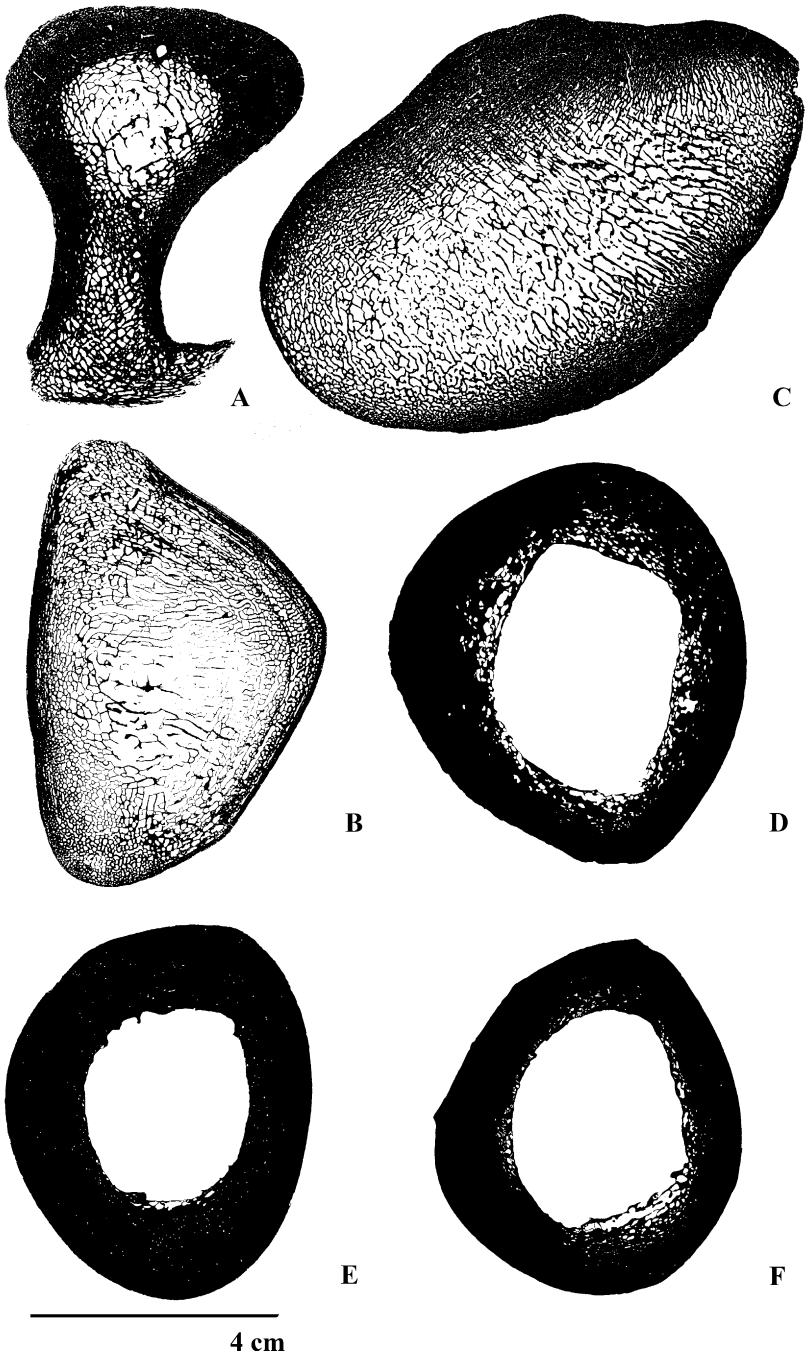


**Fig. 15.** Mid-diaphyseal cross-sections of humeri of the largest aquatic (**A–C**) and terrestrial (**A–F**) placental mammals. Taxa are arranged according to their lifestyle and phylogenetic affinities. Taxa illustrated are: **(A)** *Otaria flavescens*; **(B)** *Mirounga leonina*; **(C)** Cetotheriidae (genus and species unknown, from the Turonian, Miocene); **(D–E)** *Bison bison*; **(F)** *Bison bonasus*. Scale: 4 cm.

**Fig. 15.** Coupes transversales mi-diaphysaires d'humérus des plus grands mammifères placentaires aquatiques (**A–C**) et terrestres (**D–F**). Les taxons sont disposés selon leur mode de vie et leur ordre dans la phylogénie. Les taxons représentés sont : **(A)** *Otaria flavescens* ; **(B)** *Mirounga leonina* ; **(C)** Cetotheriidae (genre et espèce indéterminés, du Turonien, Miocène) ; **(D–E)** *Bison bison* ; **(F)** *Bison bonasus*. Échelle : 4 cm.

*maturus* and *Palorchestes* (Oxnard, 1993; de Buffrénil et al., 2010).

The humerus of chelonians shows no habitat-specific pattern, as noted above for the tibia and radius (Fig. 17). Humeri of all sampled chelonians have an extensive spongiosa that occludes the medullary region and a generally thick cortex, even in terrestrial species.

In diapsids, the humerus was sampled only in amphibious and terrestrial taxa. Small terrestrial squamates (Fig. 18A–H) generally have a thin but compact cortex,

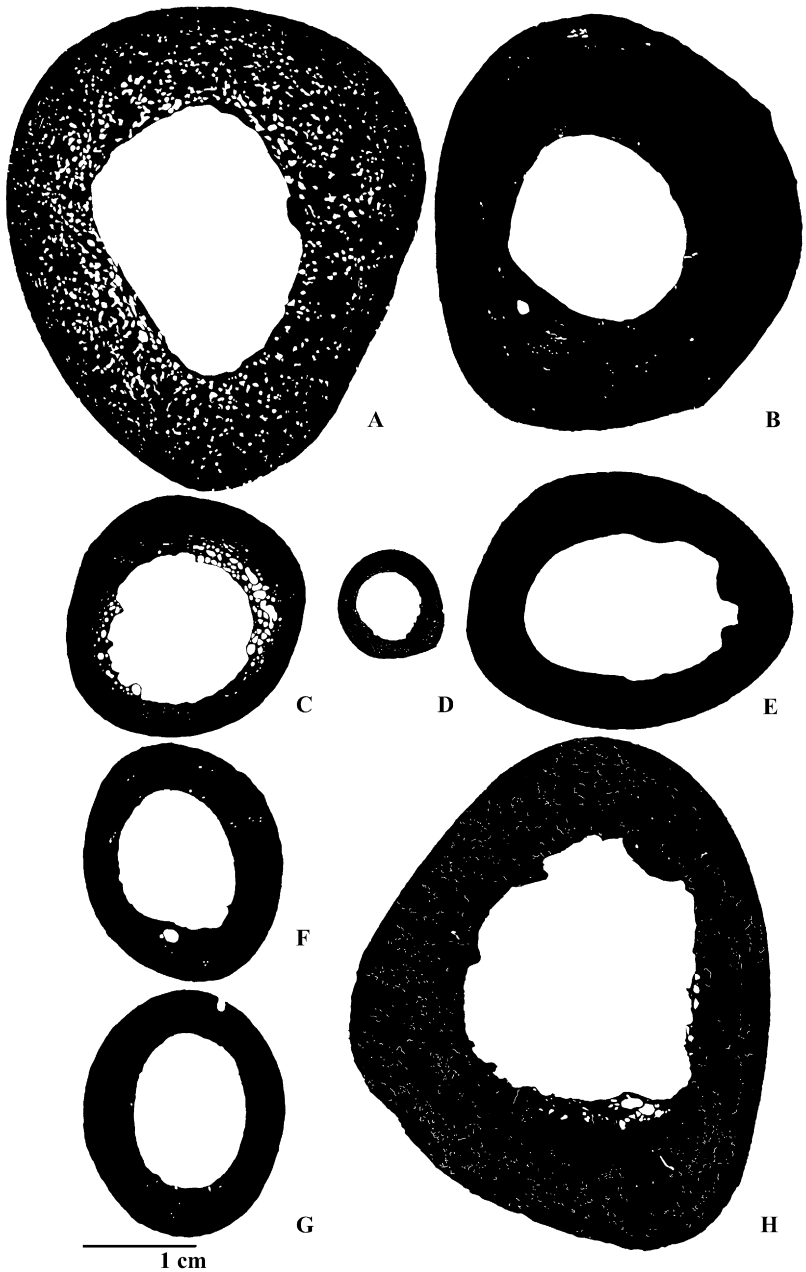


**Fig. 16.** Mid-diaphyseal cross-sections of humeri of large terrestrial ruminants. Taxa are arranged according to their lifestyle and phylogenetic affinities. Taxa illustrated are: **(A)** *Taurotragus oryx*; **(B)** *Boselaphus tragocamelus*; **(C)** *Rangifer tarandus*; **(D)** *Capreolus capreolus*, **(E)** *Cervus elaphus*; **(F)** *Dama dama*; **(G)** *Axis axis*; **(H)** *Syncerus caffer*. Scale: 1 cm.

**Fig. 16.** Coupes transversales mi–diaphysaires d'humérus de ruminants terrestres de grande taille. Les taxons sont disposés selon leur mode de vie et leur ordre dans la phylogénie. Les taxons représentés sont : **(A)** *Taurotragus oryx* ; **(B)** *Boselaphus tragocamelus* ; **(C)** *Rangifer tarandus* ; **(D)** *Capreolus capreolus* ; **(E)** *Cervus elaphus* ; **(F)** *Dama dama* ; **(G)** *Axis axis* ; **(H)** *Syncerus caffer*. Échelle : 1 cm.

with the exception of *Gerrhonotus imbricatus* (Fig. 18H), that displays a thick cortex, as for the radius (Fig. 11D). Mid-sized terrestrial squamates (Fig. 18J–N) also show a thin, compact cortex. Of all squamates sampled here, only *Varanus griseus* (Fig. 18N) has moderately well-developed vascularization, presumably reflecting the higher maximal metabolic rate of varanids than of other squamates (Clemente et al., 2009). The sole amphibious squamate sampled, *Amblyrhynchus cristatus* (Fig. 18I) has a thick, compact cortex. The other amphibious sampled diapsid, *Crocodylus siamensis* (Fig. 18O) has a thick, densely vascularized cortex.

## 6. Discussion

The illustrations described above may perhaps help paleobiologists, especially those reluctant to use quantitative methods, to infer the lifestyle of extinct stego-

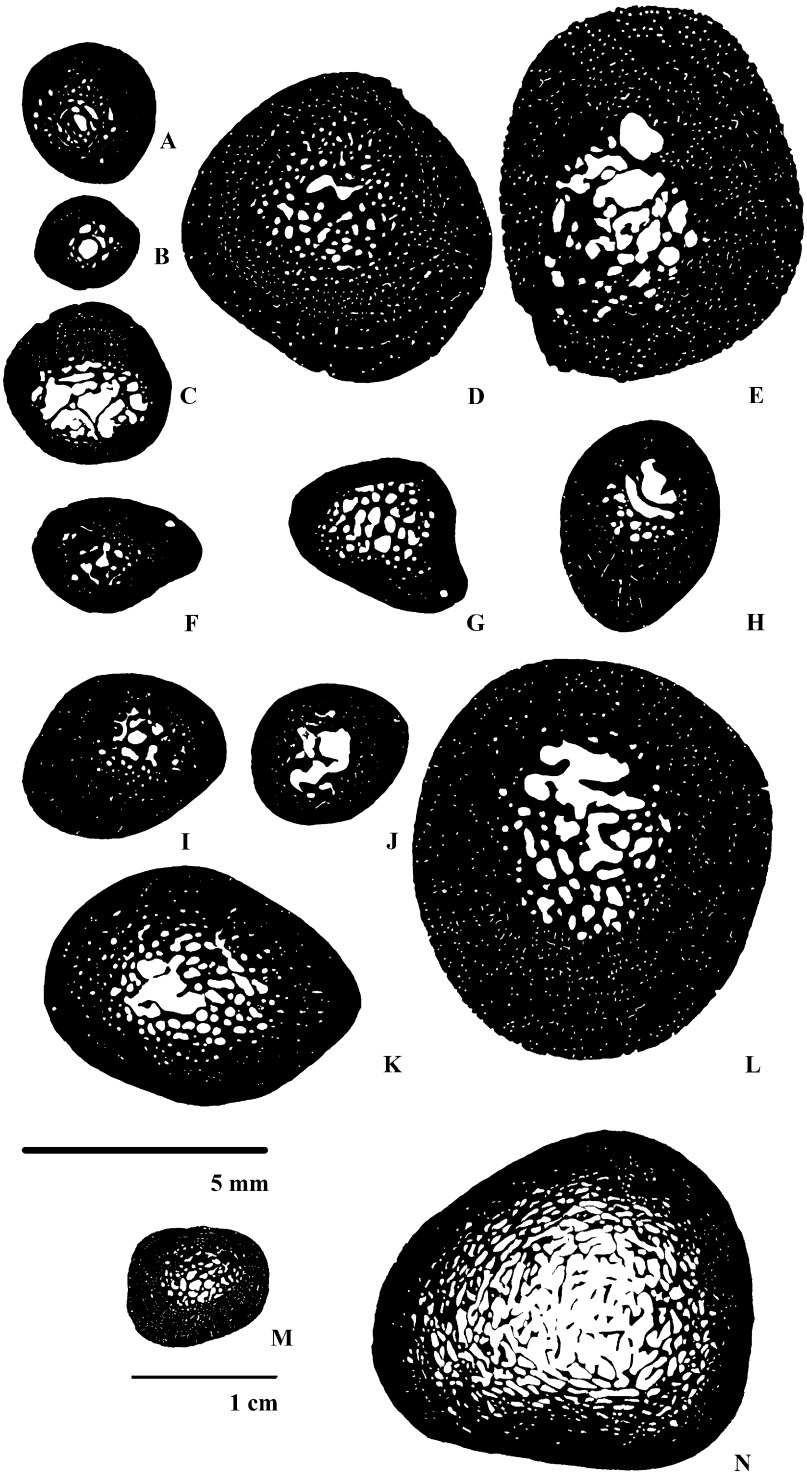


**Fig. 17.** Mid-diaphyseal cross-sections of humeri of medium-sized (**A–L**) and large (**M–N**) aquatic (**A–J**) and terrestrial (**K–N**) testudines. Taxa are arranged according to their lifestyle and phylogenetic affinities. Taxa shown are: **(A)** *Pelusios subniger*; **(B)** *Pelusios niger*; **(C)** *Pelomedusa subrufa*; **(D)** *Erymnochelys madagascariensis*; **(E)** *Chelydra serpentina*; **(F–G)** *Emys orbicularis*; **(H)** *Malaclemys terrapin*; **(I)** *Trachemys scripta*; **(J)** *Kinosternon* sp.; **(K)** *Testudo graeca*; **(L)** *Geochelone carbonaria*; **(M)** *Geochelone radiata;* **(N)** *Cylindraspis indica*. Scale: (**A–L**): 5 mm; (**M–N**): 1 cm.

**Fig. 17.** Coupes transversales mi-diaphysaires d'humérus de tortues de tailles moyenne (**A–L**) et grande (**M–N**), de mode de vie aquatique (**A–J**) et terrestre (**K–N**). Les taxons sont disposés selon leur mode de vie et leur ordre dans la phylogénie. Les taxons représentés sont : **(A)** *Pelusios subniger*; **(B)** *Pelusios niger* ; **(C)** *Pelomedusa subrufa* ; **(D)** *Erymnochelys madagascariensis* ; **(E)** *Chelydra serpentina* ; **(F–G)** *Emys orbicularis* ; **(H)** *Malaclemys terrapin* ; **(I)** *Trachemys scripta* ; **(J)** *Kinosternon* sp. ; **(K)** *Testudo graeca* ; **(L)** *Geochelone carbonaria* ; **(M)** *Geochelone radiata* ; **(N)** *Cylindraspis indica*. Échelle : (**A–L**) : 5 mm; (**M–N**) : 1 cm.

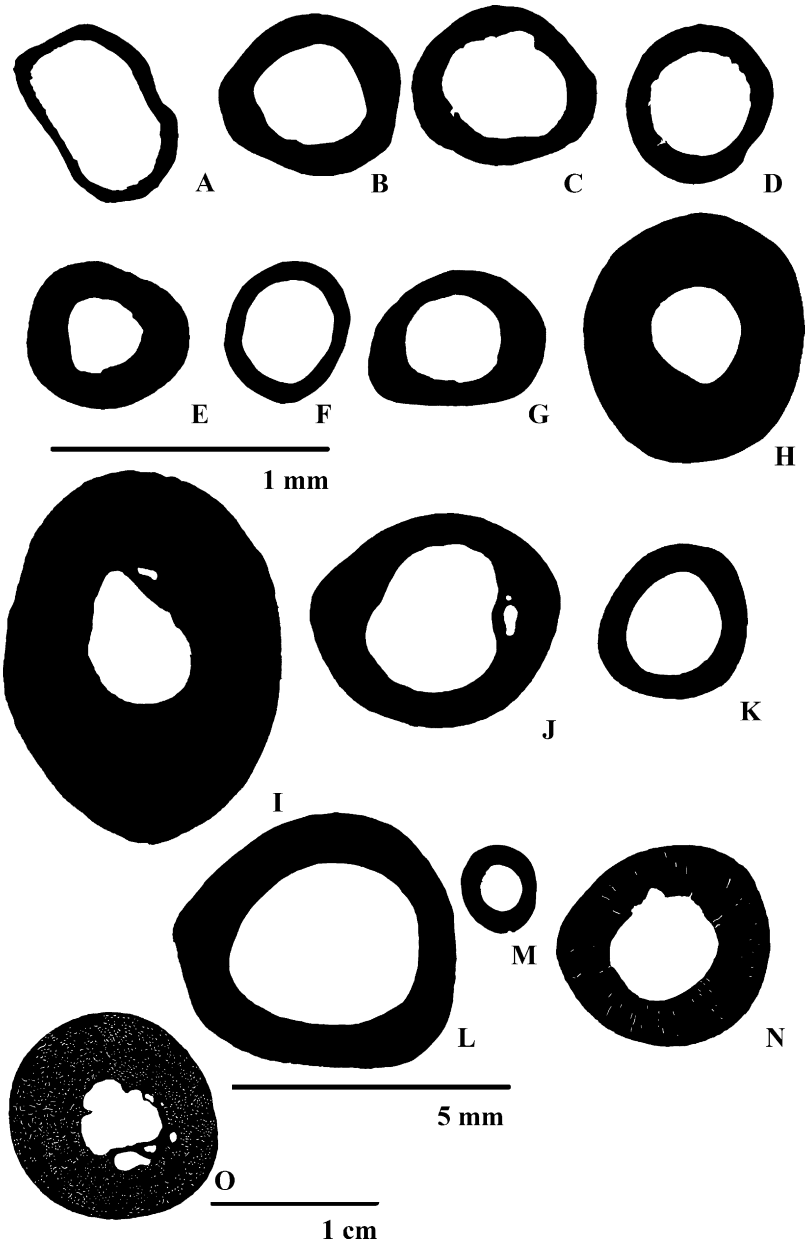


**Fig. 18.** Mid-diaphyseal cross-sections of humeri of small (**A–H**), medium-sized (**I–N**), and large (**O**), amphibious (**I**, **O**), and terrestrial (**A–H**; **J–N**) diapsids. Taxa are arranged according to the maximal diameter of the sections, their lifestyle and phylogenetic affinities. Taxa illustrated are: **(A)** *Sceloporus horridus horridus*; **(B)** *Sceloporus grammicus microlepidotus*; **(C)** *Sceloporus gadoviae*; **(D)** *Urosaurus bicarinatus bicarinatus*; **(E)** *Urosaurus bicarinatus anonymorphus*; **(F)** *Coleonyx elegans*; **(G)** *Cnemidophorus deppei*; **(H)** *Gerrhonotus imbricatus*; **(I)** *Amblyrhynchus cristatus*; **(J)** *Ctenosaura pectinata*; **(K–L)** *Iguana iguana*; **(M)** *Gerrhonotus viridiflavana*; **(N)** *Varanus griseus*; **(O)** *Crocodylus siamensis*. Scale: (**A–H**): 1 mm; (**I–N**): 5 mm; (**O**): 1 cm.

**Fig. 18.** Coupes transversales mi-diaphysaires d'humérus de diapsides de petite (**A–H**), moyenne (**I–N**) et grande (**O**) tailles, amphibies (**I**, **O**) ou terrestres (**A–H; J–N**). Les taxons sont disposés selon le diamètre maximal des sections, leur mode de vie et leur ordre dans la phylogénie. Les taxons représentés sont : **(A)** *Sceloporus horridus horridus* ; **(B)** *Sceloporus grammicus microlepidotus* ; **(C)** *Sceloporus gadoviae* ; **(D)** *Urosaurus bicarinatus bicarinatus* ; **(E)** *Urosaurus bicarinatus anonymorphus* ; **(F)** *Coleonyx elegans*; **(G)** *Cnemidophorus deppei* ; **(H)** *Gerrhonotus imbricatus* ; **(I)** *Amblyrhynchus cristatus* ; **(J)** *Ctenosaura pectinata* ; **(K–L)** *Iguana iguana* ; **(M)** *Gerrhonotus viridiflavana* ; **(N)** *Varanus griseus* ; **(O)** *Crocodylus siamensis*. Échelle : (**A–H**) : 1 mm; (**I–N**) : 5 mm; (**O**) : 1 cm.

cephalians (sensu Laurin, 1998). However, they also show that paleobiological inference on that basis alone is occasionally misleading because exceptions appear to break every rule, as is all too common in biology. One of the most notable exceptions noted above is the humerus of the zadypodid *Zaedyus pichiy*, that looks superficially like that of a small aquatic to amphibious mammal. The possible link with fossoriality would be worth investigating with a larger taxonomic sample of fossorial mammals. Similarity in phenotypes (at the microanatomical level) between at least some fossorial and aquatic mammals would require reassessing some paleobiological inferences based on such

data and might allow to better discriminate between both alternatives. For instance, an aquatic (Canoville and Laurin, 2010; Ray et al., 2005) or burrowing (Retallack et al., 2003) lifestyle has been suggested for the Permo-Triassic dicynodont *Lystrosaurus* from South Africa, although serious doubts have been expressed about the data supporting a fossorial lifestyle (Modesto and Botha–Brink, 2010).

The drawings also show why our inference models (Canoville and Laurin, 2010; Germain and Laurin, 2005; Kriloff et al., 2008) are more successful at discriminating aquatic tetrapods from amphibious and terrestrial ones: aquatic tetrapods (Fig. 3A, 5A) differ most from the others, as a visual inspection of the sections shows. Amphibious taxa differ less from terrestrial ones in their long bone microanatomy, and for this reason, amphibious and terrestrial tetrapods are more difficult to discriminate from each other on that basis.

The paleobiological inferences that we previously drew from long bone microanatomy generated interest (e.g. Clack and Klembara, 2009; Nesbitt et al., 2009), but use of some of our previous work is hampered by the fact that the inference models were not made easily accessible. Here, we rectify this problem by providing easy-to-use Excel spreadsheets into which bone compactness profile data can be entered to obtain lifestyle inferences. We provide one (SOM 1) for the amniote radius, and one (SOM 2) for the tetrapod tibia. These should be used to obtain inferences of taxa within the body-size range (indicated in the spreadsheets) that is represented in the taxonomic sample used to produce the models because body size is known to include lifestyle information (Canoville and Laurin, 2010; Germain and Laurin, 2005). To know more about the taxonomic sampling underlying these inference models, see our papers on these datasets (Germain and Laurin, 2005; Kriloff et al., 2008). Inference models based on the humerus of lissamphibian (Canoville and Laurin, 2009) and amniotes (Canoville and Laurin, 2010) and on the lissamphibian femur (Laurin et al., 2009) were previously published and are not included here.

## Acknowledgments

We thank Peggy Vincent and Aurélie Kriloff for having drawn most of the tibial cross-sections, and Martine Sache for having drawn some of the radial sections. We also thank all people who lent specimens for this study. This includes J. Castanet (UPMC; Université Pierre & Marie Curie), Elizabeth Chadwick (Cardiff School of Biomedical Sciences), V. de Buffrénil (MNHN), H. Francillon-Vieillot (U. Paris 7), S. Godfrey (Calvert marine Museum, Maryland), C. Miaud (U. de Savoie) T. Mörs, E. Pellée (MNHN), F. Renoult (MNHN), V. H. Reynoso-Rosales (UNAM; Universidad Nacional Autonoma de Mexico), D. Robineau (MNHN), U. Johansson (Swedish Museum of Natural History, Stockholm), and A. S. Severtsov (Moscow State University). Many of the sections were prepared by M.-M. Loth (U. Paris 7) or H. Lamrous (Collège de France). Jean-Sébastien Steyer and an anonymous referee made constructive comments that improved the text. This research was financed by the CNRS (UMR 7207), by a French Ministry of Research doctoral grant to A. C., and by two SYNTHESYS grants (AT–TAF–628 and 1437) to M. L.

## Appendix A. Inference model for the amniote radius (Germain and Laurin 2005)

This can be used for any amniote with a radius of a section diameter ranging from 0.35 to 43 mm (see Supplementary material).

## Appendix B. Inference model for the tetrapod tibia (Kriloff et al. 2008)

This can be used for any tetrapodomorph crownward of *Eusthenopteron* with a tibial of a section diameter ranging from 0.25 to 40 mm (see Supplementary material).

## Appendix. Supplementary material

There is supplementary material supplied with the electronic version of this article doi:10.1016/j.crpv.2011.02.003.

## References

Canoville, A., Laurin, M., 2009. Microanatomical diversity of the humerus and lifestyle in lissamphibians. Acta. Zool. 90, 110–122.
Canoville, A., Laurin, M., 2010. Evolution of humeral microanatomy and lifestyle in amniotes, and some comments on paleobiological inferences. Biol. J. Linn. Soc. 100, 384–406.
Castanet, J., Curry Rogers, K., Cubo, J., Boisard, J.–J., 2000. Periosteal bone growth rates in extant ratites (ostriche and emu). Implications for assessing growth in dinosaurs. C. R. Acad. Sci. Paris, Ser. III. 323, 543–550.
Clack, J.A., Klembara, J., 2009. An articulated specimen of *Chroniosaurus dongusensis* and the morphology and relationships of the chroniosuchids. Spec. Pap. Palaeontol. 81, 15–42.
Clemente, C.J., Withers, P.C., Thompson, G.G., 2009. Metabolic rate and endurance capacity in Australian varanid lizards (Squamata: Varanidae: Varanus). Biol. J. Linn. Soc. 97, 664–676.
Cubo, J., Ponton, F., Laurin, M., de Margerie, E., Castanet, J., 2005. Phylogenetic signal in bone microstructure of sauropsids. Syst. Biol. 54, 562–574.
de Buffrénil, V., Schoevaert, D., 1988. On how the periosteal bone of the delphinid humerus becomes cancellous: ontogeny of a histological specialization. J. Morph. 198, 149–164.
de Buffrénil, V., Mazin, J.-M., 1990. Bone histology of the ichthyosaurs: comparative data and functional interpretation. Paleobiology. 16, 435–447.
de Buffrénil, V., Mazin, J.-M., 1993. Some aspects of skeletal growth in Triassic and post–Triassic ichthyosaurs as revealed by bone histology. In: Pinna, G., Mazin, J.-M. (Eds.), Evolution, ecology and biogeography of the Triassic reptiles. Paleontologia Lombarda della Società Italiana di Scienze Naturali e del Museo Civico di Storia Naturale di Milano, Nuova serie, Milan, pp. 63–68.
de Buffrénil, V., Mazin, J.-M., de Ricqlès, A., 1987. Caractères structuraux et mode de croissance du fémur d'*Omphalosaurus nisseri*, ichthyosaurien du Trias moyen de Spitsberg. Ann. Paleontol. 73, 195–216.
de Buffrénil, V., Canoville, A., D'Anastasio, R., Doming, D.P., 2010. Evolution of sirenian pachyosteosclerosis, a model–case for the study of bone structure in aquatic tetrapods. J. Mammal. Evol. 17, 101–120.
de Ricqlès, A., 1974a. Recherches paléohistologiques sur les os longs des tétrapodes V. – Cotylosaures et mésosaures. Ann. Paleontol. 60, 171–216.
de Ricqlès, A., 1974b. Recherches paléohistologiques sur les os longs des tétrapodes IV. – Eothériodontes et pélycosaures. Ann. Paleontol. 60, 1–39.

de Ricqlès, A., de Buffrénil, V., 2001. Bone histology, heterochronies and the return of tetrapods to life in water: w[h]ere are we? In: Mazin, J.-M., de Buffrénil, V. (Eds.), Secondary Adaptation of Tetrapods to Life in Water. Verlag Dr F Pfeil, München, pp. 289–306.

deBraga, M., Rieppel, O., 1997. Reptile phylogeny and the interrelationships of turtles. Zool. J. Linn. Soc. 120, 281–354.

Desdevises, Y., Legendre, P., Azouzi, L., Morand, S., 2003. Quantifying phylogenetically structured environmental variation. Evolution. 57, 2467–2652.

Felsenstein, J., 1985. Phylogenies and the comparative method. Am. Nat. 125, 1–15.

Fish, F.E., Stein, B.R., 1991. Functional correlates of differences in bone density among terrestrial and aquatic genera in the family Mustelidae (Mammalia). Zoomorphology 110, 339–345.

Fröbisch, N.B., Schoch, R.R., 2009. The largest specimen of *Apateon* and the life history pathway of neoteny in the Paleozoic temnospondyl family Branchiosauridae. Fossil. Rec. 12, 83–90.

Frost, D.R., Grant, T., Faivovich, J., Bain, R.H., Haas, A., Haddad, C.F.B., de Sá, R.O., Channing, A., Wilkinson, M., Donnellan, S.C., Raxworthy, C.J., Campbell, J.A., Blotto, B., Moler, P., Drewes, R.C., Nussbaum, R.A., Lynch, J.D., Green, D.M., Wheeler, W.C., 2006. The amphibian tree of life. Bull. Am. Mus. Nat. Hist. 297, 1–370.

Hanken, J., 1999. Larvae in amphibian development and evolution. In: The Origin and Evolution of Larval Forms. Academic Press, London, pp. 61–108.

Germain, D., Laurin, M., 2005. Microanatomy of the radius and lifestyle in amniotes (Vertebrata Tetrapoda). Zoologica. Scr. 34, 335–350.

Girondot, M., Laurin, M., 2003. Bone Profiler: a tool to quantify, model and statistically compare bone section compactness profiles. J. Vertebr. Paleontol. 23, 458–461.

Gregory, T.R., 2003. Variation across amphibian species in the size of the nuclear genome supports a pluralistic, hierarchical approach to the C–value enigma. Biol. J. Linn. Soc. 79, 329–339.

Hedges, S.B., Poling, L.L., 1999. A molecular phylogeny of reptiles. Science 283, 998–1001.

Hugall, A.F., Foster, R., Lee, M.S.Y., 2007. Calibration choice, rate smoothing, and the pattern of tetrapod diversification according to the long nuclear gene RAG–1. Syst. Biol. 56, 543–563.

Iwabe, N., Hara, Y., Kumazawa, Y., Shibamoto, K., Saito, Y., Miyata, T., Katoh, K., 2005. Sister group relationship of turtles to the bird–crocodilian clade revealed by nuclear DNA–coded proteins. Mol. Biol. Evol. 22, 810–813.

Jørgensen, C.B., 2000. Amphibian respiration and olfaction and their relationships: from Robert Townson (1794) to the present. Biol. Rev. 75, 297–345.

Kriloff, A., Germain, D., Canoville, A., Vincent, P., Sache, M., Laurin, M., 2008. Evolution of bone microanatomy of the tetrapod tibia and its use in palaeobiological inference. J. Evol. Biol. 21, 807–826.

Larivière, S., 2003. *Amblonyx cinereus*. Mammal. Spec., 1–5.

Laurin, M., 1998. The importance of global parsimony and historical bias in understanding tetrapod evolution. Part II. Vertebral centrum, costal ventilation, and paedomorphosis. Ann. Sci. Nat. Zool. 13 (Ser 19), 99–114.

Laurin, M., 2000. Seymouriamorphs. In: Heatwole, H., Carroll, R.L. (Eds.), Amphibian Biology. Surrey Beatty & Sons, Chipping Norton, pp. 1064–1080.

Laurin, M., 2008. Systématique. In: paléontologie et biologie évolutive moderne: l'exemple de la sortie des eaux des vertébrés. Ellipses, Paris, 176 p.

Laurin, M., Reisz, R.R., 1995. A reevaluation of early amniote phylogeny. Zool. J. Linn. Soc. 113, 165–223.

Laurin, M., Girondot, M., Loth, M.–M., 2004. The evolution of long bone microanatomy and lifestyle in lissamphibians. Paleobiology 30, 589–613.

Laurin, M., Germain, D., Steyer, J.–S., Girondot, M., 2006. Données microanatomiques sur la conquête de l'environnement terrestre par les vertébrés. C. R. Palevol. 5, 603–618.

Laurin, M., Canoville, A., Quilhac, A., 2009. Use of paleontological and molecular data in supertrees for comparative studies: the example of lissamphibian femoral microanatomy. J. Anat. 215, 110–123.

Lee, M.S.Y., 1997. Reptile relationships turn turtle. Nature 389, 245–246.

Lee, M.S.Y., 2001. Molecules, morphology, and the monophyly of diapsid reptiles. Contrib. Zool. 70, 1–18.

Legendre, P., 2000. Comparison of permutation methods for the partial correlation and partial Mantel tests. J. Statist. Comput. Simul. 67, 37–73.

Lyson, T.R., Bever, G.S., Bhullar, B.–A.S., Joyce, W.G., Gauthier, J.A., 2010. Transitional fossils and the origin of turtles. Biol. Lett. [Published online].

Mantel, N., 1967. The detection of disease clustering and a generalized regression approach. Cancer. Res. 27, 209–220.

Modesto, S.P., Botha–Brink, J., 2010. A burrow cast with *Lystrosaurus* skeletal remains from the Lower Triassic of South Africa. Palaios. 25, 274–281.

Mukherjee, D., Ray, S., Sengupta, D.P., 2010. Preliminary observations on the bone microstructure, growth patterns, and life habits of some Triassic temnospondyls from India. J. Vertebr. Paleontol. 30, 78–93.

Nesbitt, S., Stocker, M.R., Small, B., Downs, A., 2009. The osteology and relationships of *Vancleavea campi* (Reptilia: Archosauriformes). Zool. J. Linn. Soc. 157, 814–864.

Nopcsa, F.B., Heidsieck, E., 1934. Über eine pachyostotische Rippe aus der kreide Rügens. Acta. zool. Stockh. XV., 431–455.

Oxnard, C.E., 1993. Bone and bones, architecture and stress, fossils and osteoporosis. J. Biomech. 26 (Suppl. 1), 63–79.

Ray, S., Chinsamy, A., Bandyopadhyay, S., 2005. *Lystrosaurus murrayi* (Therapsida Dicynodontia): bone histology, growth and lifestyle adaptations. Palaeontology 48, 1169–1185.

Reisz, R.R., Laurin, M., 1991. *Owenetta* and the origin of turtles. Nature 349, 324–326.

Retallack, G.J., Smith, R.M.H., Ward, P.D., 2003. Vertebrate extinction across Permian–Triassic boundary in Karoo Basin South Africa. GSA. Bulletin 115, 1133–1152.

Rieppel, O., Reisz, R.R., 1999. The origin and early evolution of turtles. Annu. Rev. Ecol. Syst. 30, 1–22.

Scheyer, T.M., Sander, P.M., 2007. Shell bone histology indicates terrestrial palaeoecology of basal turtles. Proc. R. Soc. Lond. B. 274, 1885–1893.

Stein, B.R., 1989. Bone density and adaptation in semiaquatic mammals. J. Mammal. 70, 467–476.

Sterli, J., 2010. Phylogenetic relationships among extinct and extant turtles: the position of Pleurodira and the effects of the fossils on rooting crown–group turtles. Contrib. Zool. 79, 93–106.

Steyer, J.–S., Laurin, M., Castanet, J., de Ricqlès, A., 2004. First histological and skeletochronological data on temnospondyl growth; palaeoecological and palaeoclimatological implications. Palaeogeogr. Palaeoclimatol. Palaeoecol. 206, 193–201.

Wall, W.P., 1983. The correlation between high limb–bone density and aquatic habits in recent mammals. J. Paleont. 57, 197–207.

Werneburg, I., Sánchez–Villagra, M.R., 2009. Timing of organogenesis support basal position of turtles in the amniote tree of life. BMC. Evol. Biol. 9, 82.

Wiffen, J., de Buffrénil, V., de Ricqlès, A., Mazin, J.–M., 1995. Ontogenetic evolution of bone structure in Late Cretaceous Plesiosauria from New Zealand. Geobios 28, 625–640.